

# Mechanical Properties of Polymer Solids and Liquids

# 4

*With a name like yours, you might be any shape, almost.*  
—Lewis Carroll, *Through the Looking Glass*

## 4.1 Introduction

Polymers are in general use because they provide good mechanical properties at reasonable cost. The efficient application of macromolecules requires at least a basic understanding of the mechanical behavior of such materials and the factors that influence this behavior.

The mechanical properties of polymers are not single-valued functions of the chemical nature of the macromolecules. They will vary also with molecular weight, branching, cross-linking, crystallinity, plasticizers, fillers and other additives, orientation, and other consequences of processing history and sometimes with the thermal history of the particular sample.

When all these variables are fixed for a particular specimen, it will still be observed that the properties of the material will depend strongly on the temperature and time of testing compared, say, to metals. This dependence is a consequence of the viscoelastic nature of polymers. Viscoelasticity implies that the material has the characteristics both of a viscous liquid which cannot support a stress without flowing and an elastic solid in which removal of the imposed stress results in complete recovery of the imposed deformation.

Although the mechanical response of macromolecular solids is complex, it is possible to gain an understanding of the broad principles that govern this behavior. Polymeric articles can be designed rationally, and polymers can be synthesized for particular applications. This chapter summarizes the salient factors that influence some important properties of solid polymers.

## 4.2 Thermal Transitions

All liquids contract as their temperatures are decreased. Small, simple molecules crystallize quickly when they are cooled to the appropriate temperatures. Larger

and more complex molecules must undergo translational and conformational reorganizations to fit into crystal lattices and their crystallization rates may be so reduced that a rigid, amorphous glass is formed before extensive crystallization occurs on cooling. In many cases, also, the structure of polymers is so irregular that crystalline structures cannot be formed. If crystallization does not occur, the viscosity of the liquid will increase on cooling to a level of  $10^{14}$  Ns/m<sup>2</sup> ( $10^{15}$  poises) where it becomes an immobile glass. Conformational changes associated with normal volume contraction or crystallization can no longer take place in the glassy state and the thermal coefficient of expansion of the material falls to about one-third of its value in the warmer, liquid condition.

Most micromolecular species can exist in the gas, liquid, or crystalline solid states. Some can also be encountered in the glassy state. The behavior of glass-forming high polymers is more complex, because their condition at temperatures slightly above the glassy condition is more accurately characterized as rubbery than liquid. Unvulcanized elastomers described in Section 4.5 are very viscous liquids that will flow gradually under prolonged stresses. If they are cross-linked in the liquid state, this flow can be eliminated. In any case these materials are transformed into rigid, glassy products if they are cooled sufficiently. Similarly, an ordinarily glassy polymer like polystyrene is transformed into a rubbery liquid on warming to a high enough temperature.

The change between rubbery liquid and glassy behavior is known as the glass transition. It occurs over a temperature range, as shown in Fig. 4.1, where the temperature–volume relations for glass formation are contrasted with that for crystallization. Line *ABCD* is for a substance that crystallizes completely. Such a material undergoes an abrupt change in volume and coefficient of thermal expansion at its melting point  $T_m$ . Line *ABEG* represents the cooling curve for a glass-former. Over a short temperature range corresponding to the interval *EF*, the thermal coefficient of expansion of the substance changes but there is no discontinuity in the volume–temperature curve. By extrapolation, as shown, a temperature  $T'_g$  can be located that may be regarded as the glass transition temperature for the particular substance at the given cooling rate. If the material is cooled more slowly, the volume–temperature curve is like *ABEG'* and the glass transition temperature  $T''_g$  is lower than in the previous case. The precise value of  $T_g$  will depend on the cooling rate in the particular experiment.

Low-molecular-weight molecules melt and crystallize completely over a sharp temperature interval. Crystallizable polymers differ in that they melt over a range of temperatures and do not crystallize completely, especially if they have high molecular weights. Figure 4.2 compares the volume–temperature relation for such a polymer with that for an uncrystallizable analog. Almost all crystallizable polymers are considered to be “semicrystalline” because they contain significant fractions of poorly ordered, amorphous chains. Note that the melting region in this sketch is diffuse, and the melting point is identified with the temperature at B, where the largest and most perfect crystallites would melt. The noncrystalline portion of this material exhibits a glass transition temperature, as shown. It

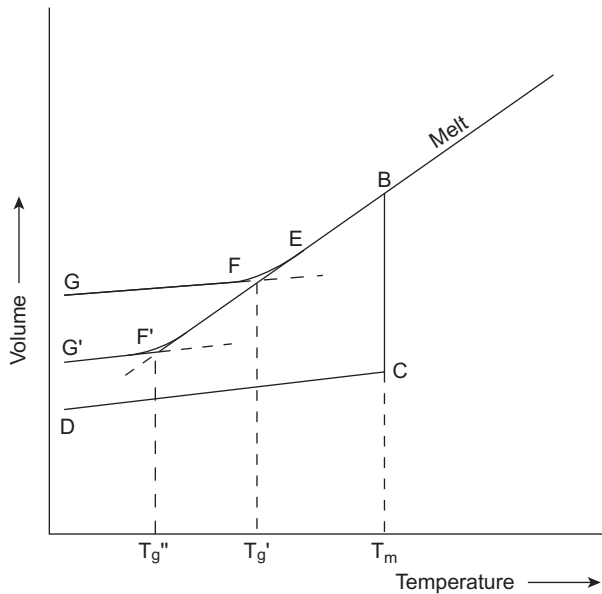


**FIGURE 4.1**

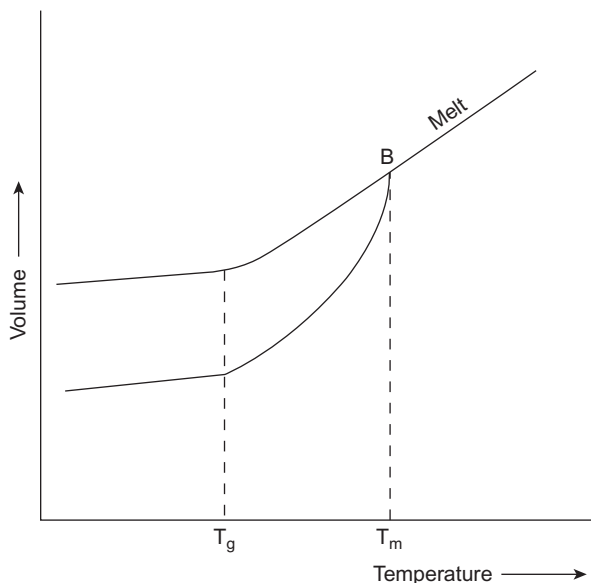
Volume-temperature relations for a glass-forming polymer and a material that crystallizes completely on cooling.  $T_m$  is a melting point, and  $T_g'$  and  $T_g''$  are glass transition temperatures of an uncrystallized material that is cooled quickly and slowly, respectively.

appears that  $T_g$  is characteristic generally of amorphous regions in polymers, whether or not other portions of the material are crystalline.

The melting range of a semicrystalline polymer may be very broad. Branched (low-density) polyethylene is an extreme example of this behavior. Softening is first noticeable at about 75 °C although the last traces of crystallinity do not disappear until about 115 °C. Other polymers, like nylon-6,6, have much narrower melting ranges.

Measurements of  $T_m$  and melting range are conveniently made by thermal analysis techniques like differential scanning calorimetry (dsc). The value of  $T_m$  is usually taken to be the temperature at which the highest melting crystallites disappear. This parameter depends to some extent on the thermal history of the sample since more perfect, higher melting crystallites are produced by slower crystallization processes in which more time is provided for the conformational changes needed to fit macromolecular segments into the appropriate crystal pattern.

The onset of softening is usually measured as the temperature required for a particular polymer to deform a given amount under a specified load. These values are known as *heat deflection temperatures*. Such data do not have any direct connection with results of X-ray, thermal analysis, or other measurements of the melting of crystallites, but they are widely used in designing with plastics.

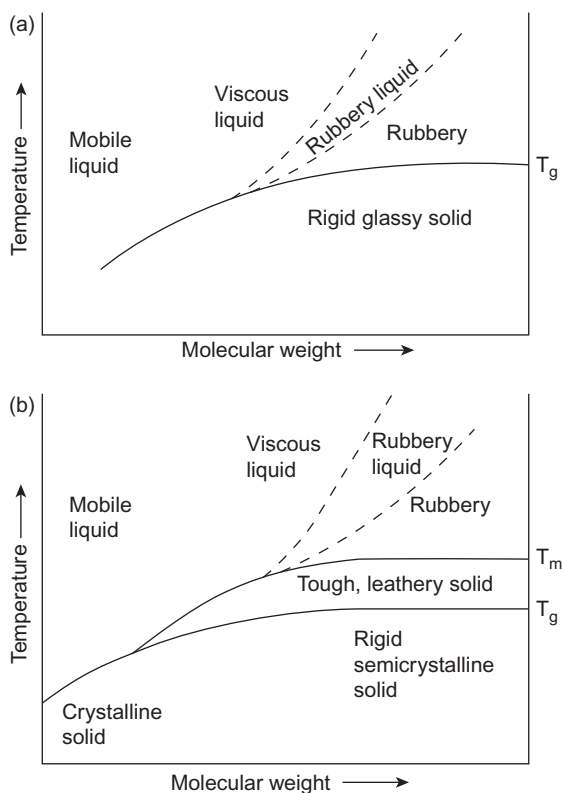


**FIGURE 4.2**

Volume—temperature relation for an amorphous (upper line) polymer and semicrystalline (lowerline) polymer.

Both  $T_m$  and  $T_g$  are practically important.  $T_g$  sets an upper temperature limit for the use of amorphous thermoplastics like poly(methyl methacrylate) or polystyrene and a lower temperature limit for rubbery behavior of an elastomer like SBR rubber or 1,4-*cis*-polybutadiene. With semicrystalline thermoplastics,  $T_m$  or the onset of the melting range determines the upper service temperature. Between  $T_m$  and  $T_g$ , semicrystalline polymers tend to be tough and leathery. Brittleness begins to set in below  $T_g$  of the amorphous regions although secondary transitions below  $T_g$  are also important in this connection. As a general rule, however, semicrystalline plastics are used at temperatures between  $T_g$  and a practical softening temperature that lies above  $T_g$  and below  $T_m$ .

Changes in temperature and polymer molecular weight interact to influence the nature and consequences of thermal transitions in macromolecules. Warming of glassy amorphous materials converts them into rubbery liquids and eventually into viscous liquids. The transition between these latter states is very ill marked, however, as shown in Fig. 4.3a. Enhanced molecular weights increase  $T_g$  up to a plateau level, which is encountered approximately at  $\overline{DP}_n = 500$  for vinyl polymers. The rubbery nature of the liquid above  $T_g$  becomes increasingly more pronounced with higher molecular weights. Similar relations are shown in Fig. 4.3b for semicrystalline polymers where  $T_m$  at first increases and then levels off as the molecular weight of the polymer is made greater.  $T_m$  depends on the

**FIGURE 4.3**

Approximate relations between temperature, molecular weight, and physical state for (a) an amorphous polymer and (b) a semicrystalline polymer.

size and perfection of crystallites. Chain ends ordinarily have different steric requirements from interchain units, and the ends will either produce lattice imperfections in crystallites or will not be incorporated into these regions at all. In either case,  $T_m$  is reduced when the polymer contains significant proportions of lower molecular weight species and hence of chain ends.

## 4.3 Crystallization of Polymers

*Order is Heaven's first law.*

—Alexander Pope, *Essay on Man*

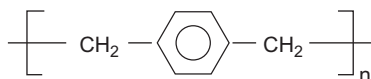
Sections of polymer chains must be capable of packing together in ordered periodic arrays for crystallization to occur. This requires that the macromolecules be

fairly regular in structure. Random copolymerization will prevent crystallization. Thus, polyethylene would be an ideal elastomer except for the fact that its very regular and symmetrical geometry permits the chains to pack together closely and crystallize very quickly. To inhibit crystallization and confer elastomeric properties on this polymer, ethylene is commonly copolymerized with substantial proportions of another olefin or with vinyl acetate.

A melting temperature range is observed in all semicrystalline polymers, because of variations in the sizes and perfection of crystallites. The crystal melting point is the highest melting temperature observed in an experiment like differential scanning calorimetry. It reflects the behavior of the largest, defect-free crystallites. For high-molecular-weight linear polyethylene this temperature, labeled  $T_m$ , is about 141 °C. Other regular, symmetrical polymers will have lower or higher melting points depending on chain flexibility and interchain forces. At equilibrium at the melting point, the Gibbs free-energy change of the melting process,  $\Delta G_m$ , is zero and

$$T_m = \Delta H_m / \Delta S_m \quad (4-1)$$

The conformations of rigid chains will not be much different in the amorphous state near  $T_m$  than they are in the crystal lattice. This means that the melting process confers relatively little additional disorder on the system;  $\Delta S_m$  is low and  $T_m$  is increased correspondingly. For example, ether units in poly(ethylene oxide) (1-42) make this structure more flexible than polyethylene, and the  $T_m$  of high-molecular-weight versions of the former species is only 66 °C. By contrast, poly(*p*-xylene) (4-1) is composed of stiff chains and its crystal melting point is 375 °C.



4-1

Stronger intermolecular forces result in greater  $\Delta H_m$  values and an increase in  $T_m$ . Polyamides, which are hydrogen bonded, are higher melting than polyolefins with the same degree of polymerization, and the melting points of polyamides decrease with increasing lengths of hydrocarbon sequences between amide groupings. Thus the  $T_m$  of nylon-6 and nylon-11 are 225 and 194 °C, respectively.

Bulky side groups in vinyl polymers reduce the rate of crystallization and the ability to crystallize by preventing the close approach of different chain segments. Such polymers require long stereoregular configurations (Section 1.12.2) in order to crystallize.

Crystal perfection and crystallite size are influenced by the rate of crystallization, and  $T_m$  is affected by the thermal history of the sample. Crystals grow in size by accretion of segments onto stable nuclei. These nuclei do not exist at temperatures above  $T_m$ , and crystallization occurs at measurable rates only at

temperatures well below the melting point. As the crystallization temperature is reduced, this rate accelerates because of the effects of increasing concentrations of stable nuclei. The rate passes eventually through a maximum, because the colder conditions reduce the rate of conformational changes needed to place polymer segments into proper register on the crystallite surfaces. When  $T_g$  is reached, the crystallization rate becomes negligible. For isotactic polystyrene, for example, the rate of crystallization is a maximum at about 175 °C. Crystallization rates are zero at 240 °C ( $T_m$ ) and at 100 °C ( $T_g$ ). If the polystyrene melt is cooled quickly from temperatures above 240 °C to 100 °C or less, there will be insufficient time for crystallization to occur and the solid polymer will be amorphous. The isothermal crystallization rate of crystallizable polymers is generally a maximum at temperatures about halfway between  $T_g$  and  $T_m$ .

Crystallinity should be distinguished from molecular orientation. Both phenomena are based on alignment of segments of macromolecules but the crystalline state requires a periodic, regular placement of the atoms of the chain relative to each other whereas the oriented molecules need only be aligned without regard to location of atoms in particular positions. Orientation tends to promote crystallization because it brings the long axes of macromolecules parallel and closer together. The effects of orientation can be observed, however, in uncrystallized regions of semicrystalline polymers and in polymers that do not crystallize at all.

### 4.3.1 Degree of Crystallinity

High-molecular-weight flexible macromolecules do not crystallize completely. When the polymer melt is cooled, crystallites will be nucleated and start to grow independently throughout the volume of the specimen. If polymer chains are long enough, different segments of the same molecule can be incorporated in more than one crystallite. When these segments are anchored in this fashion the intermediate portions of the molecule may not be left with enough freedom of movement to fit into the lattice of a crystallite. It is also likely that regions in which threadlike polymers are entangled will not be able to meet the steric requirements for crystallization.

Several methods are available for determining the average crystallinity of a polymer specimen. One technique relies on the differences between the densities of completely amorphous and entirely crystalline versions of the same polymer and estimates crystallinity from the densities of real specimens, which are intermediate between these extremes. Crystalline density can be calculated from the dimensions of the unit cell in the crystal lattice, as determined by X-ray analysis. The amorphous density is measured with solid samples which have been produced by rapid quenching from melt temperatures, so that there is no experimental evidence of crystallinity. Polyethylene crystallizes too rapidly for this expedient to be effective (the reason for this is suggested in [Section 4.3.2.1](#)), and volume–temperature relations of the melt like that in [Fig. 4.1](#) are extrapolated in order to estimate the amorphous density at the temperature of interest. Crystalline regions

have densities on the average about 10% higher than those of amorphous domains, since chain segments are packed more closely and regularly in the former.

The density method is very convenient, because the only measurement required is that of the density of a polymer sample. It suffers from some uncertainties in the assignments of crystalline and amorphous density values. An average crystallinity is estimated as if the polymer consisted of a mixture of perfectly crystalline and completely amorphous regions. The weight fraction of material in the crystalline state  $w_c$  is estimated assuming that the volumes of the crystalline and amorphous phases are additive:

$$w_c = \rho_c(\rho - \rho_a) / \rho(\rho_c - \rho_a) \quad (4-2)$$

where  $\rho$ ,  $\rho_c$ , and  $\rho_a$  are the densities of the particular specimen, perfect crystal, and amorphous polymer, respectively. Alternatively, if additivity of the masses of the crystalline and amorphous regions is assumed, then the volume fraction  $\phi_c$  of polymer in the crystalline state is estimated from the same data:

$$\phi_c = (\rho - \rho_a) / (\rho_c - \rho_a) \quad (4-3)$$

X-ray measurements can be used to determine an average degree of crystallinity by integrating the intensities of crystalline reflections and amorphous halos in diffraction photographs. Broadline nuclear magnetic resonance (NMR) spectroscopy is also suitable for measuring the ratio of amorphous to crystalline material in a sample because mobile components of the polymer in amorphous regions produce narrower signals than segments that are immobilized in crystallites. The composite spectrum of the polymer specimen is separated into crystalline and amorphous components to assign an average crystallinity. Infrared absorption spectra of many polymers contain bands which are representative of macromolecules in crystalline and in amorphous regions. The ratio of absorbances at characteristically crystalline and amorphous frequencies can be related to a crystalline/amorphous ratio for the specimen. An average crystallinity can also be inferred from measurements of the enthalpy of fusion per unit weight of polymer when the specific enthalpies of the crystalline and amorphous polymers at the melting temperature can be estimated. This method, which relies on differential scanning calorimetry, is particularly convenient and popular.

Each of the methods cited yields a measure of average crystallinity, which is really only defined operationally and in which the polymer is assumed artificially to consist of a mixture of perfectly ordered and completely disordered segments. In reality, there will be a continuous spectrum of structures with various degrees of order in the solid material. Average crystallinities determined by the different techniques cannot always be expected to agree very closely, because each method measures a different manifestation of the structural regularities in the solid polymer.

A polymer with a regular structure can attain a higher degree of crystallinity than one that incorporates branches, configurational variations, or other features that cannot be fitted into crystallites. Thus linear polyethylene can be induced to

**Table 4.1** Representative Degrees of Crystallinity (%)

Low-density polyethylene	45–74
High-density polyethylene	65–95
Polypropylene fiber	55–60
Poly(ethylene terephthalate) fiber	20–60
Cellulose (cotton)	60–80

crystallize to a greater extent than the branched polymer. However, the degree of crystallinity and the mechanical properties of a particular crystallizable sample depend not only on the polymer structure but also on the conditions under which crystallization has occurred.

Quenching from the amorphous melt state always produces articles with lower average crystallinities than those made by slow cooling through the range of crystallization temperatures. If quenched specimens are stored at temperatures higher than the glass transition of the polymer, some segments in the disordered regions will be mobile enough to rearrange themselves into lower energy, more ordered structures. This phenomenon, which is known as *secondary crystallization*, will result in a progressive increase in the average crystallinity of the sample.

For the reasons given, a single average crystallinity level cannot be assigned to a particular polymer. Certain ranges of crystallinity are fairly typical of different macromolecular species, however, with variations due to polymer structure, methods for estimating degree of crystallinity, and the histories of particular specimens. Some representative crystallinity levels are listed in Table 4.1. The ranges listed for the olefin polymers in this table reflect variations in average crystallinities which result mainly from different crystallization histories. The range shown for cotton specimens is due entirely to differences in average values measured by X-ray, density, and other methods, however, and this lack of good coincidence of different estimates is true to some extent also of polyester fibers.

Crystallization cannot take place at temperatures below  $T_g$ , and  $T_m$  is therefore always at a higher temperature than  $T_g$ . The presence of a crystalline phase in a polymer extends its range of mechanical usefulness compared to strictly amorphous versions of the same species. In general, an increased degree of crystallinity also reduces the solubility of the material and increases its rigidity. The absolute level of crystallinity that a polymer sample can achieve depends on its structure, but the actual degree of crystallinity, which is almost always less than this maximum value, will also reflect the crystallization conditions.

### 4.3.2 Microstructure of Semicrystalline Polymers

When small molecules crystallize, each granule often has the form of a crystal grown from a single nucleus. Such crystals are relatively free of defects and have well-defined crystal faces and cleavage planes. Their shapes can be related to the

geometry of the unit cell of the crystal lattice. Polymers crystallized from the melt are polycrystalline. Their structures are a conglomerate of disordered material and clusters of crystallites that developed more or less simultaneously from the growth of many nuclei. Distinct crystal faces cannot be distinguished, and the ordered regions in semicrystalline polymers are generally much smaller than those in more perfectly crystallized micromolecular species. X-ray maxima are broadened by small crystallite sizes and by defects in larger crystals. In either case such data may be interpreted as indicating that the highly ordered regions in semicrystalline polymers have dimensions of the order of  $10^{-5}$ – $10^{-6}$  cm. These domains are held together by “tie molecules” which traverse more than one crystallite. This is what gives a semicrystalline polymer its mechanical strength. Aggregates of crystals of small molecules are held together only by secondary forces and are easily split apart. Such fragility is not observed in a polymer sample unless the ordered regions are large enough to swallow most macromolecules whole and leave few interregional molecular ties.

The term *crystallite* is used in polymer science to imply a component of an interconnected microcrystalline structure. Metals also belong to the class of microcrystalline solids, since they consist of tiny ordered grains connected by strong boundaries.

#### 4.3.2.1 Nucleation of Crystallization

Crystallization begins from a nucleus that may derive from surfaces of adventitious impurities (heterogeneous nucleation) or from the aggregation of polymer segments at temperatures below  $T_m$  (homogeneous nucleation). The latter process is reversible up to the point where a critical size is reached, beyond which further growth results in a net decrease of free energy of the system. Another source of nuclei in polymer melts is ordered regions that are not fully destroyed during the prior melting process. Such nuclei can occur if segments in ordered regions find it difficult to diffuse away from each other, because the melt is very viscous or because these segments are pinned between regions of entanglement. The dominant effect in bulk crystallization appears to be the latter type of nucleation, as evidenced by in nuclear magnetic resonance spectroscopy relaxation experiments and other observations that indicate that polyolefins contain regions with different segmental densities at temperatures above their melting temperatures [1–3]. Although segments of macromolecules in the most compact of these regions are not crystalline, as measured by calorimetry or X-ray diffraction, they would remain close together even when the bulk of the polymer is molten and can reform crystallites very readily when the temperature is lowered. The number of such nuclei that are available for crystal growth is a function of the degree of supercooling of the polymer. Incidentally, this explains why polyethylene has never been observed in the completely amorphous state; even when the melt is quenched in liquid  $N_2$  crystallites will form since they are produced simply by the shrinkage of the polymer volume on cooling. An alternative mechanism that is postulated involves heterogeneous nucleation on adventitious impurities.

The nature of such adventitious nuclei has not been clearly established. The growing crystal has to be able to wet its nucleus, and it has been suggested that the surfaces of the effective heterogeneities contain crevices in which crystalline polymer is trapped.

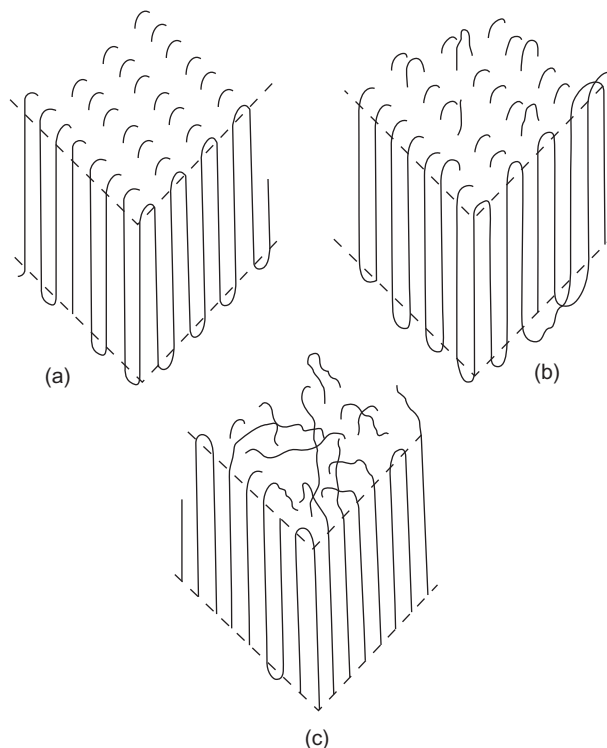
The control of nucleation density can be important in many practical applications. A greater number of nucleation sites results in the formation of more ordered regions, each of which has smaller overall dimensions. The average size of such domains can affect many properties. An example is the transparency of packaging films made from semicrystalline polymers. The refractive indexes of amorphous and crystalline polymer domains differ, and light is refracted at their boundaries. Films will appear hazy if the sizes of regions with different refractive indexes approach the wavelength of light. Nucleating agents are sometimes deliberately added to a polymer to increase the number of nuclei and reduce the dimensions of ordered domains without decreasing the average degree of crystallinity. Such agents are generally solids with colloidal dimensions, like silica and various salts. Sometimes a higher melting semicrystalline polymer will nucleate the crystallization of another polymer. Blending with small concentrations of isotactic polypropylene ( $T_m, 176\text{ }^\circ\text{C}$ ) improves the transparency of sheets and films of polyethylene ( $T_m, 115\text{--}137\text{ }^\circ\text{C}$ ), for example.

#### 4.3.2.2 *Crystal Lamellae*

Once nucleated, crystallization proceeds with the growth of folded chain ribbon-like crystallites called lamellae. The arrangement of polymer chains in the lamellae has some resemblance to that in platelike single crystals which can be produced by precipitating crystallizable polymers from their dilute solutions. In such single crystals the molecules are aligned along the thinnest dimension of the plate. The lengths of extended macromolecules are much greater than the thickness of these crystals and it is evident that a polymer chain must fold outside the plate volume and reenter the crystallite at a different point. When polymer single crystals are carefully prepared, it is found that the dimensions are typically a few microns ( $1\text{ }\mu\text{m} = 1\text{ micron} = 10^{-6}\text{ m}$ ) for the length and breadth and about  $0.1\text{ }\mu\text{m}$  for the thickness. The thickness is remarkably constant for a given set of crystallization conditions but increases with the crystallization temperature. Perfect crystallinity is not achieved, because the portions of the chains at the surfaces and in the folds are not completely ordered.

There is uncertainty about the regularity and tightness of the folds in solution-grown single crystals. Three models of chain conformations in a single crystal are illustrated in Fig. 4.4.

Folded-chain crystals grow by extension of the length and breadth but not the thickness. The supply of polymer segments is much greater in the melt than in dilute solution, and crystallization in the bulk produces long ribbonlike folded chain structures. These lamellae become twisted and split as a result of local depletion of crystallizable material and growth around defect structures. The

**FIGURE 4.4**

Possible conformations of polymer chains at the surfaces of chain-folded single crystals. (a) Adjacent reentry model with smooth, regular chain folds, (b) adjacent reentry model with rough fold surface, and (c) random reentry (switchboard) model.

regularity of chain folding and reentry is very likely much less under these conditions than in the single crystals produced by slow crystallization from dilute solution.

Another major difference in crystallization from the melt and from dilute solution is that neighboring growing lamellae will generally be close together under the former conditions. Segments of a single molecule are thus likely to be incorporated in different crystallites in bulk crystallized polymer. These “tie molecules” bind the lamellae together and make the resulting structure tough. The number of tie molecules increases with increasing molecular weight and with faster total crystallization rates. The crystallization rate is primarily a function of the extent of supercooling. Cooler crystallization temperatures promote more nuclei but retard the rates of conformational changes required for segmental placement on growing nuclei. (It is observed empirically that the maximum rate of isothermal crystallization occurs at about  $0.8T_m$ , where the maximum crystal melting

temperature  $T_m$  is expressed in K degrees.) The impact resistance and other mechanical characteristics of semicrystalline polymers are dependent on crystallization conditions. The influence of fabrication conditions on the quality of articles is much more pronounced with semicrystalline polymers than with metals or other materials of construction, as a consequence.

#### 4.3.2.3 Morphology of Semicrystalline Polymers

The morphology of a crystallizable polymer is a description of the forms that result from crystallization and the aggregation of crystallites. The various morphological features that occur in bulk crystallized polymers are reviewed in this section.

Crystalline lamellae are the basic units in the microstructures of solid semicrystalline polymers. The lamellae are observed to be organized into two types of larger structural features depending on the conditions of the bulk solidification process.

The major feature of polymers that have been bulk crystallized under quiescent conditions are polycrystalline structures called *spherulites*. These are roughly spherical supercrystalline structures which exhibit Maltese cross extinction patterns when examined under polarized light in an optical microscope. Spherulites are characteristic of semicrystalline polymers and are also observed in low-molecular-weight materials that have been crystallized from viscous media. Spherulites are aggregates of lamellar crystallites. They are not single crystals and include some disordered material within their boundaries. The sizes of spherulites may vary from somewhat greater than a crystallite to dimensions visible to the naked eye.

A spherulite is built up of lamellar subunits that grow outward from a common nucleus. As this growth advances into the uncrystallized polymer, local inhomogeneities in concentrations of crystallizable segments will be encountered. The folded chain fibril will inevitably twist and branch. At some early stage in its development the spherulite will resemble a sheaf of wheat, as shown schematically in Fig. 4.5a. Branching and fanning out of the growing lamellae tend to create a spherical shape, but neighboring spherulites will impinge on each other in bulk crystallized polymers and prevent the development of true spherical symmetry. The main structural units involved in a spherulite include branched, twisted lamellae with polymer chain directions largely perpendicular to their long axes and interfibrillar material, which is essentially uncrystallized. This is sketched in Fig. 4.6.

The growth of polymer spherulites involves the segregation of noncrystallizable material into the regions between the lamellar ribbons. The components that are not incorporated into the crystallites include additives like oxidation stabilizers, catalyst residues, and so on, as well as comonomer units or branches. The spherulite structures and interspherulitic boundaries are held together primarily by polymer molecules which run between the twisted lamellar subunits and the spherulites themselves. Slow crystallization at low degrees of supercooling

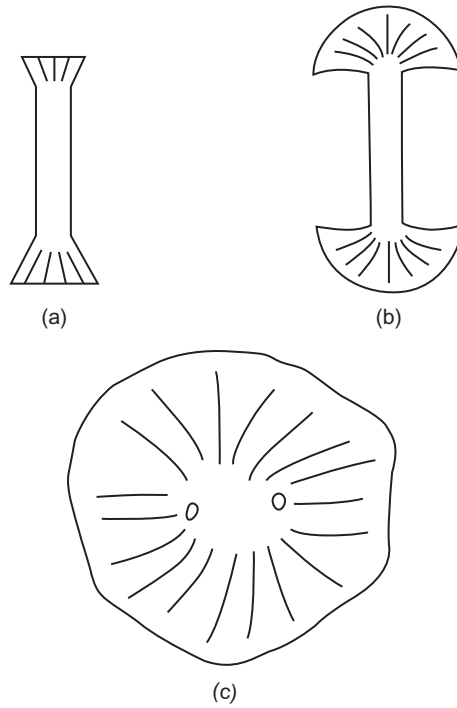


**FIGURE 4.5**  
Successive stages in the development of a spherulite by fanning growth from a nucleus.

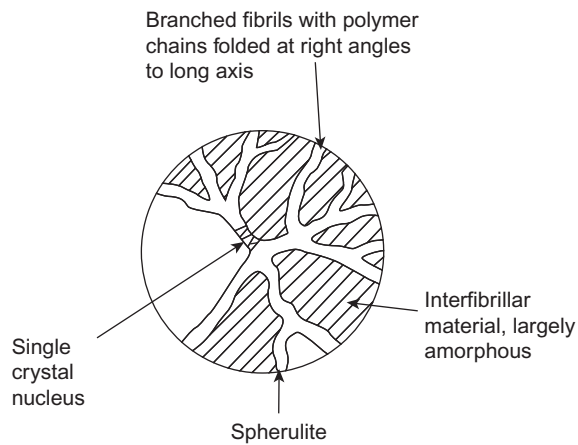


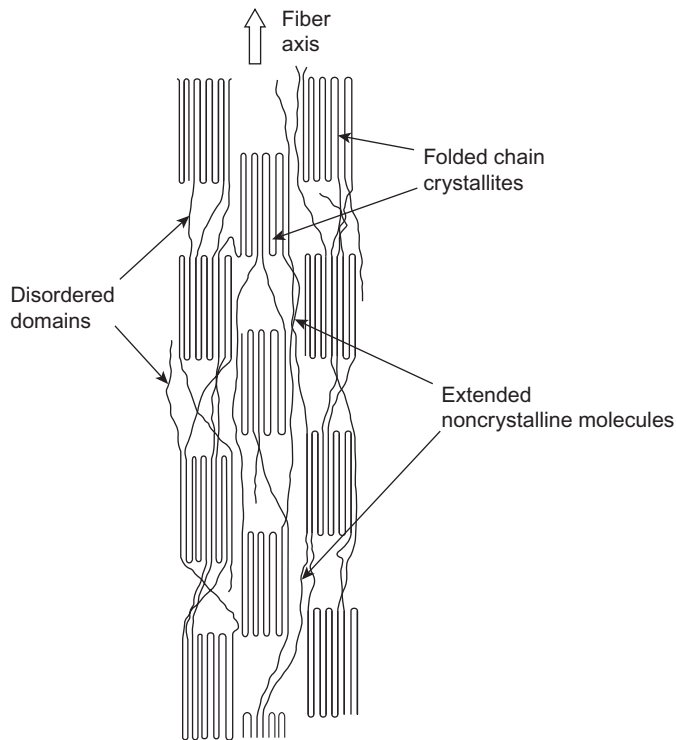
**FIGURE 4.6**  
Basic structure of a polymer spherulite.

produces fewer nuclei and larger spherulites. The polymeric structures produced under such conditions are more likely to be brittle than if they were produced by faster cooling from the melt. This is because there will be fewer interspherulitic tie molecules and because low-molecular-weight uncrystallizable matter will have had more opportunity to diffuse together and produce weak boundaries between spherulites.

The supermolecular structures developed on fast cooling of crystallizable polymers change with time because of secondary crystallization. A parallel phenomenon is the progressive segregation of mobile uncrystallizable low-molecular-weight material at storage temperatures between  $T_g$  and  $T_m$ . This will also result in a gradual embrittlement of the matrix polymer. A useful way to estimate whether an additive at a given loading can potentially cause such problems over the lifetime of a finished article is to accelerate the segregation process by deliberately producing some test specimens under conditions that facilitate slow and extensive crystallization.

The type of nucleation that produces spherulitic supercrystalline structures from quiescent melts is not the same as that which occurs more typically in the industrial fabrication of semicrystalline polymer structures. The polymer molecules are under stress as they crystallize in such processes as extrusion, fiber spinning, and injection molding. The orientation of chain segments in flow under stress results in the formation of elongated crystals that are aligned in the flow direction. These are not folded chain crystallites. The overall orientation of the macromolecules in these structures is along the long crystal axis rather than transverse to it as in lamellae produced during static crystallization. Such elongated chain fibrils are probably small in volume, but they serve as a nucleus for the growth of a plurality of folded chain lamellae, which develop with their molecular axes parallel to the parent fibril and their long axes initially at right angles to the long direction of the nucleus. These features are called *row structures*, or *row-nucleated structures*, as distinguished from spherulites. Row-nucleated microstructures are as complex as spherulites and include tie molecules, amorphous regions, and imperfect crystallites. The relative amounts and detailed natures of row-nucleated and spherulitic supercrystalline structures in a particular sample of polymer are determined by the processing conditions used to form the sample. The type or organization that is produced influences many physical properties.

Other supercrystalline structures can be produced under certain conditions. A fibrillar morphology is developed when a crystallizable polymer is stretched at temperatures between  $T_g$  and  $T_m$ . (This is the orientation operation mentioned in Section 1.4). Similar fibrillar regions are produced when a spherulitically crystallized specimen is stretched. In both cases, lamellae are broken up into folded-chain blocks that are connected together in microfibrils whose widths are usually between 60 and  $200 \times 10^{-8}$  cm. In each microfibril, folded-chain blocks alternate with amorphous sections that contain chain ends, chain folds, and tie molecules. The tie molecules connecting crystalline blocks along the fiber axis direction are principally responsible for the strength of the structure. Microfibrils of this type

**FIGURE 4.7**

Schematic representation of structure of a microfibril in an oriented fiber.

make up the structure of oriented, semicrystalline, synthetic fibers. Figure 4.7 is a simplified model of such a structure. The gross fiber is made up of interwoven microfibrils that may branch, bend, and fuse together.

The mechanical properties of polymer crystallites are anisotropic. Strengths and stiffnesses along the molecular axis are those of the covalent bonds in the polymer backbone, but intermolecular cohesive forces in the transverse directions are much weaker. For example, in the chain direction the modulus of polyethylene is theoretically  $\sim 200$  GPa (i.e.,  $200 \times 10^9$  Pa), while the moduli of the crystallites in the two transverse directions are  $\sim 2$  GPa. Oriented extended chain structures are produced by very high orientations. In conventional spinning of semicrystalline fibers or monofilaments (the distinction is primarily in terms of the diameters of these products) the polymer melt is extruded and cooled, so that stretching of the solid polymer results in permanent orientation. The degree to which a high-molecular-weight polymer can be stretched in such a process is limited by the “natural draw ratio” of the polymer, which occurs because entanglements in the material prevent its extension beyond a certain extent without

breaking. These limitations are overcome industrially by so-called gel spinning. In this operation a mixture of the polymer and diluent is extruded and stretched, the diluent is removed, and the product is given a final stretch. Use of a diluent, such as a low-molecular-weight hydrocarbon in the case of polyethylene, facilitates slippage of entanglements and high elongations. Full extension of all the macromolecules in a sample requires that the ratio of the stretched to unstretched fiber lengths (draw ratio) exceeds the ratio of contour length to random coil end-to-end distance (Section 1.14.2.1). For a polyethylene of molecular weight  $10^5$  and degree of polymerization about 3600, this ratio would be 60 if the molecules behaved like fully oriented chains. When allowance is made for the effects of fixed bond angles and restricted rotational freedom on the random coil dimensions and the contour length, this ratio is calculated to be about 27. This corresponds more or less to the degrees of stretch that are achieved in the production of “superdrawn fibers” of thermoplastics, although not all the macromolecules need to be fully extended to achieve optimum properties in such materials. These products have stiffnesses and tensile strengths that approach those of glass or steel fibers. The crystal superstructures of fibers of the rodlike macromolecules mentioned in Section 4.6 are similar to those of superdrawn thermoplastics. The former do not require high draw ratios to be strong, however, because their molecules are already in a liquid crystalline order even in solution.

During high-speed extrusion processes such as those in fiber and film manufacturing processes, crystallization occurs under high gradients of pressure or temperature. The molecules in the polymer melts become elongated and oriented under these conditions, and this reduces their entropy and hence the entropy change  $\Delta S_m$  when these molecules crystallize. Since  $\Delta H_m$  is not affected, the equilibrium crystallization temperature is increased (Eq. 4-1) and nucleation and crystallization start at higher temperatures and proceed faster in such processes than in melts that are cooled under low stress or quiescent conditions.

In addition to the various morphological features listed, intermediate supermolecular structures and mixtures of these entities will be observed. The mechanical properties of finished articles will depend on the structural state of a semicrystalline polymer, and this in turn is a function of the molecular structure of the polymer and to a significant extent also of the process whereby the object was fabricated.

---

## 4.4 The Glass Transition

The mechanical properties of amorphous polymers change profoundly (three orders of magnitude) as the temperature is decreased through the glass transition region. The corresponding changes in the behavior of semicrystalline polymers are less pronounced in general, although they are also evident. At present, we do not have a complete theoretical understanding of glass transition, particularly the

molecular mechanism that is responsible for the substantial changes in mechanical properties over a fairly narrow temperature range. The glass transition appears to be a second-order transition as the heat capacity and thermal expansion coefficient of the polymer undergo finite changes. However, the glass transition temperature depends on the rate of measurement (see Section 4.4.4). Therefore, it should not be considered as a real second-order thermodynamic transition.

#### 4.4.1 Modulus–Temperature Relations

At sufficiently low temperatures a polymer will be a hard, brittle material with a modulus greater than  $10^9 \text{ N m}^{-2}$  ( $10^{10} \text{ dyn/cm}^2$ ). This is the glassy region. The tensile modulus is a function of the polymer temperature and is a useful guide to mechanical behavior. Figure 4.8 shows a typical modulus–temperature curve for an amorphous polymer.

In the glassy region the available thermal energy ( $RT$  energy units/mol) is insufficient to allow rotation about single bonds in the polymer backbone, and movements of large-scale (about 50 consecutive chain atoms) segments of macromolecules cannot take place. When a material is stressed, it can respond by deforming in a nonrecoverable or in an elastic manner. In the former case there must be rearrangements of the positions of whole molecules or segments of molecules that result in the dissipation of the applied work as internal heat. The mechanism whereby the imposed work is absorbed irreversibly involves the flow of

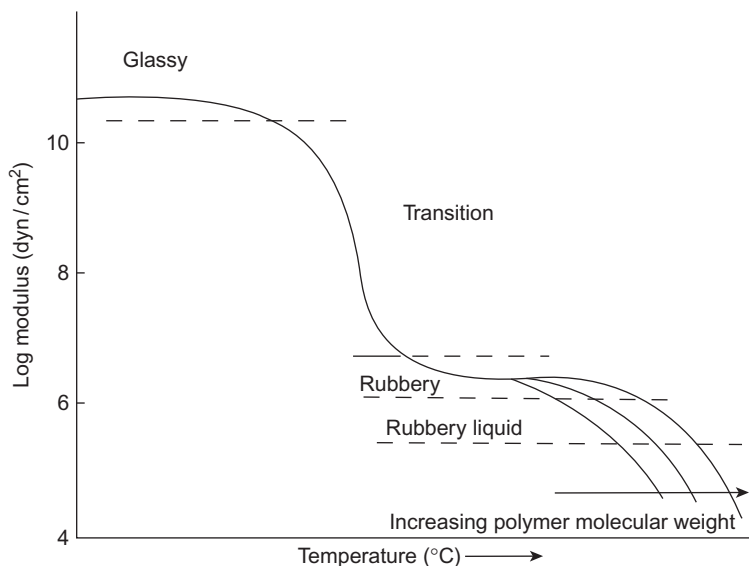


**FIGURE 4.8**

Modulus–temperature relations for an amorphous polymer.

sections of macromolecules in the solid specimen. The alternative, elastic response is characteristic of glasses, in which the components cannot flow past each other. Such materials usually fracture in a brittle manner at small deformations, because the creation of new surfaces is the only means available for release of the strain energy stored in the solid (window glass is an example). The glass transition region is a temperature range in which the onset of motion on the scale of molecular displacements can be detected in a polymer specimen. An experiment will detect evidence of such motion (Section 4.4.4) when the rate of molecular movement is appropriate to the time scale of the experiment. Since the rate of flow always increases with temperature, it is not surprising that techniques that stress the specimen more quickly will register higher transition temperatures. For a typical polymer, changing the time scale of loading by a factor of 10 shifts the apparent  $T_g$  by about 7 °C. In terms of more common experience, a plastic specimen that can be deformed in a ductile manner in a slow bend test may be glassy and brittle if it is struck rapidly at the same temperature.

As the temperature is raised the thermal agitation becomes sufficient for segmental movement and the brittle glass begins to behave in a leathery fashion. The modulus decreases by a factor of about  $10^3$  over a temperature range of about 10–20 °C in the glass-to-rubber transition region.

Let us imagine that measurement of the modulus involves application of a tensile load to the specimen and measurement of the resulting deformation a few seconds after the sample is stressed. In such an experiment a second plateau region will be observed at temperatures greater than  $T_g$ . This is the rubbery plateau. In the temperature interval of the rubbery plateau, the segmental displacements that give rise to the glass transition are much faster than the time scale of the modulus measurement, but the flow of whole macromolecules is still greatly restricted. Such restrictions can arise from primary chemical bonds as in cross-linked elastomers (Section 4.5.1) or by entanglements with other polymer chains in uncross-linked polymers. Since the number of such entanglements will be greater the higher the molecular weight of the polymer, it can be expected that the temperature range corresponding to the rubbery plateau in uncross-linked polymers will be extended to higher values of  $T$  with increasing  $M$ . This is shown schematically in Fig. 4.8. A cross-plot of the molecular weight–temperature relation is given in Fig. 4.3a.

The rubbery region is characterized by a short-term elastic response to the application and removal of a stress. This is an entropy-driven elasticity phenomenon of the type described in Section 4.5. Polymer molecules respond to the gross deformation of the specimen by changing to more extended conformations. They do not flow past each other to a significant extent, because their rate of translation is restricted by mutual entanglements. A single entangled molecule has to drag along its attached neighbors or slip out of its entanglement if it is to flow. The amount of slippage will increase with the duration of the applied stress, and it is observed that the temperature interval of the rubbery plateau is shortened as time between the load application and strain measurement is lengthened. Also, molecular flexibility and mobility increase with temperature, and continued warming of

the sample causes the scale of molecular motions to increase in the time scale of the experiment. Whole molecules will begin to slip their entanglements and flow during the several seconds required for this modulus experiment. The sample will flow in a rubbery manner. When the stress is released, the specimen will not contract completely back to its initial dimensions. With higher testing temperatures, the flow rate and the amount of permanent deformation observed will continue to increase.

If the macromolecules in a sample are cross-linked, rather than just entangled, the intermolecular linkages do not slip and the rubbery plateau region persists until the temperature is warm enough to cause chemical degradation of the macromolecules. The effects of cross-linking are illustrated in Fig. 4.9. A lightly cross-linked specimen would correspond to the vulcanized rubber in an automobile tire. The modulus of the material in the rubbery region is shown as increasing with temperature because the rubber is an entropy spring (cf. Fig. 1.3a and Section 4.5.2). The modulus also rises with increased density of cross-linking in accordance with Eq. (4-31). At high cross-link densities, the intermolecular linkages will be spaced so closely as to eliminate the mobility of segments of the size ( $\sim 50$  main chain bonds) involved in motions that are unlocked in the glass–rubber transition region. Then the material remains glassy at all usage temperatures. Such behavior is typical of tight network structures such as cured phenolics (Fig. 8.1).

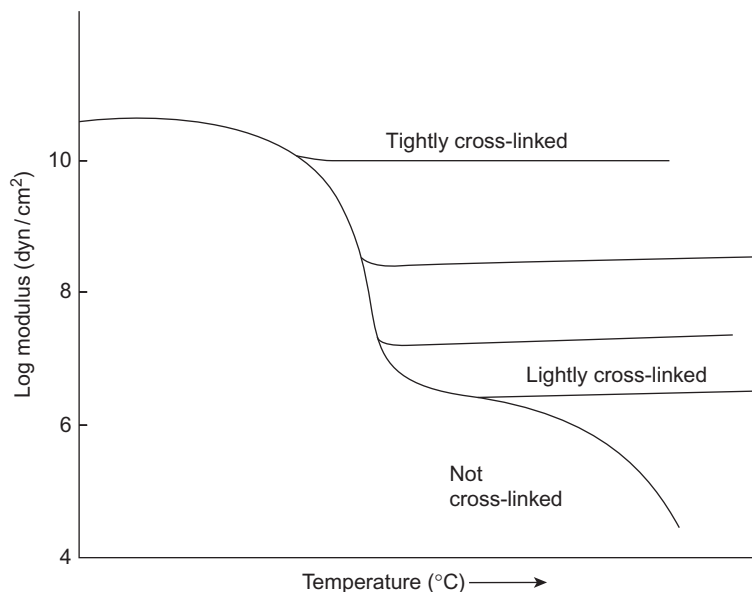


**FIGURE 4.9**

Effect of cross-linking on modulus–temperature relation for an amorphous polymer.

In a solid semicrystalline polymer, large-scale segmental motion occurs only at temperatures between  $T_g$  and  $T_m$  and only in amorphous regions. At low degrees of crystallinity the crystallites act as virtual cross-links, and the amorphous regions exhibit rubbery or glassy behavior, depending on the temperature and time scale of the experiment. Increasing levels of crystallinity have similar effects to those shown in Fig. 4.9 for variations in cross-link density. Schematic modulus–temperature relations for a semicrystalline polymer are shown in Fig. 4.10. As with moderate cross-linking, the glass transition is essentially unaffected by the presence of crystallites. At very high crystallinity levels, however, the polymer is very rigid and little segmental motion is possible. In this case the glass transition has little practical significance. It is almost a philosophical question whether a  $T_g$  exists in materials like the superdrawn thermoplastic fibers noted in Section 4.3.2.3 or the rodlike structures mentioned in Section 4.6.

The modulus–temperature behavior of amorphous polymers is also affected by admixture with plasticizers. These are the soluble diluents described briefly in Section 6.3.2. As shown in Fig. 4.11, the incorporation of a plasticizer reduces  $T_g$  and makes the polymer more flexible at any temperature above  $T_g$ . In poly(vinyl chloride), for example,  $T_g$  can be lowered from about 85 °C for unplasticized material to –30 °C for blends of the polymer with 50 wt% of dioctyl phthalate plasticizer. A very wide range of mechanical properties can be achieved with this one polymer by variations in the types and concentrations of plasticizers.

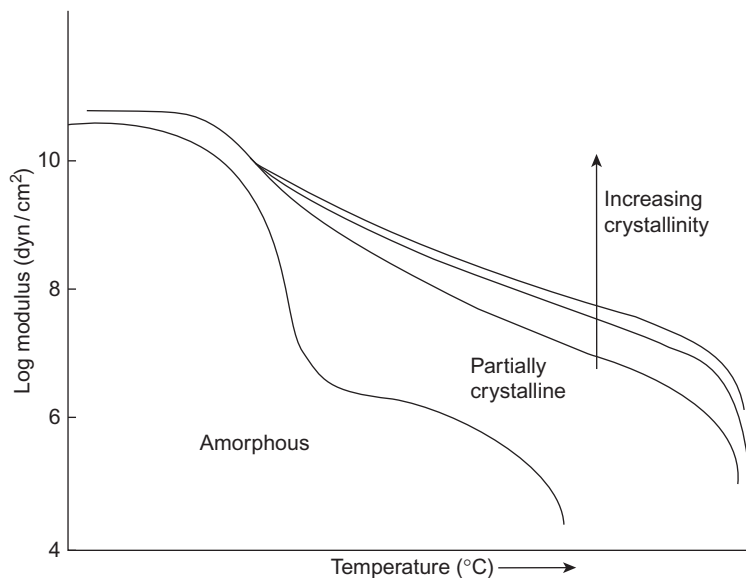


**FIGURE 4.10**

Modulus–temperature relations for amorphous and partially crystalline versions of the same polymer.

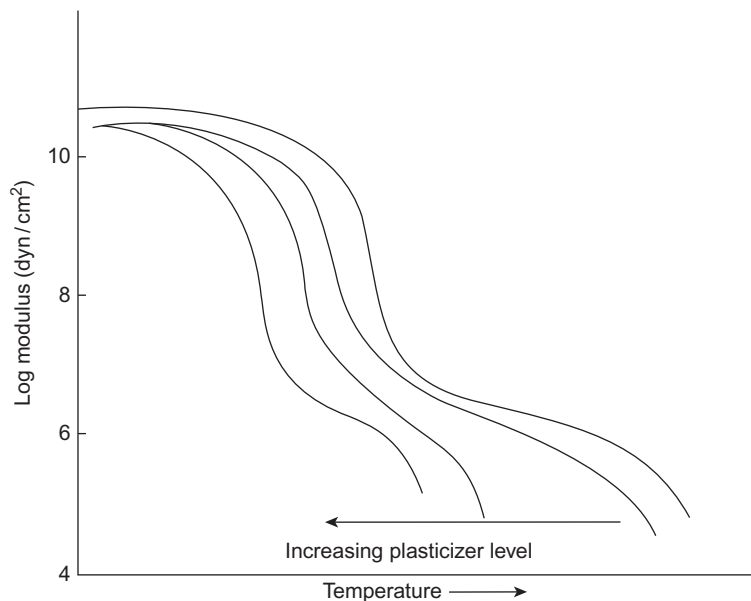


**FIGURE 4.11**

Modulus versus temperature for a plasticized amorphous polymer.

#### 4.4.2 Effect of Polymer Structure on $T_g$

Observed  $T_g$ 's vary from  $-123^\circ\text{C}$  for poly(dimethyl siloxane) (1-43) to  $273^\circ\text{C}$  for polyhydantoin (4-2) polymers used as wire enamels and to even higher temperatures for other polymers in which the main chain consists largely of aromatic structures. This range of behavior can be rationalized, and the effects of polymer structure on  $T_g$  can be predicted qualitatively. Since the glass-to-rubber transition reflects the onset of movements of sizable segments of the polymer backbone, it is reasonable to expect that  $T_g$  will be affected by the flexibility of the macromolecules and by the intensities of intermolecular forces. Table 4.2 lists  $T_g$  and  $T_m$  values for a number of polymers. The relations between intra- and interchain features of the macromolecular structure and  $T_g$  are summarized in the following paragraphs.

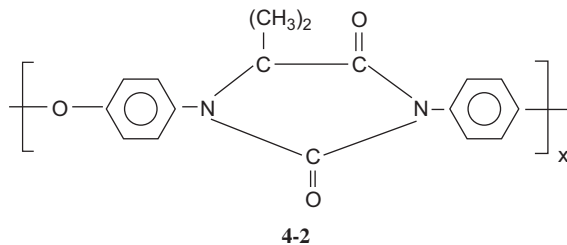
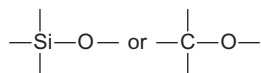


**Table 4.2** Glass Transition and Crystal Melting Temperatures of Polymers (°C)

	$T_g$	$T_m^a$		$T_g$	$T_m^a$
Poly(dimethyl siloxane)	-127	—	Poly(ethyl methacrylate)	65	—
Polyethylene	-120 <sup>b</sup>	140	Poly(propyl methacrylate)	35	—
Polypropylene(isotactic)	-8	176	Poly( <i>n</i> -butyl methacrylate)	21	—
Poly(1-butene) (isotactic)	-24	132	Poly( <i>n</i> -hexyl methacrylate)	-5	—
Polyisobutene	-73	—	Poly(phenyl methacrylate)	110	—
Poly(4-methyl-1-pentene) (isotactic)	29	250	Poly(acrylic acid)	106	—
<i>cis</i> -1,4-Polybutadiene	-102	—	Polyacrylonitrile	97	—
<i>trans</i> -1,4-Polybutadiene	-58 <sup>b</sup>	96 <sup>b</sup>	Poly(vinyl chloride) (conventional)	87	—
<i>cis</i> -1,4-Polyisoprene	-73	—	Poly(vinyl fluoride)	41	200
Polyformaldehyde	-82 <sup>b</sup>	175	Poly(vinylidene chloride)	-18	200
Polystyrene (atactic)	100	—	Poly(vinyl acetate)	32	—
Poly(alpha-methyl styrene)	168	—	Poly(vinyl alcohol)	85	—
Poly(methyl acrylate)	10	—	Polycarbonate of bisphenol A	157	—
Poly(ethyl acrylate)	-24	—	Poly(ethylene terephthalate) (unoriented)	69	267
Poly(propyl acrylate)	-37	—	Nylon-6,6 (unoriented)	50 <sup>b</sup>	265
Poly(phenyl acrylate)	57	—	Poly( <i>p</i> -xylene)	—	375
Poly(methyl methacrylate) (atactic)	105	—			

<sup>a</sup> $T_m$  is not listed for vinyl polymers in which the most common forms are atactic nor for elastomers, which are not crystalline in the unstretched state.  
<sup>b</sup>Conflicting data are reported.

The kinetic flexibility of a macromolecule is directly related to the ease with which conformational changes between *trans* and *gauche* states can take place. The lower the energy barrier  $\Delta E$  in Fig. 1.6, the greater the ease of rotation about main chain bonds. Polymers with low chain stiffnesses will have low  $T_g$ 's in the absence of complications from interchain forces. Chain backbones with



bonds tend to be flexible and have low glass transitions. Insertion of an aromatic ring in the main chain causes an increase in  $T_g$ , and this is of importance in the application of amorphous glassy polymers like poly(phenylene oxide) (1-14) and polycarbonate (1-52).

Bulky, inflexible substituents on chain carbons impede rotations about single bonds in the main chain and raise  $T_g$ . Thus, the  $T_g$  of polypropylene and poly(methyl methacrylate) are respectively higher than those of polyethylene and poly(methyl acrylate). However, the size of the substituent is not directly related to  $T_g$ ; a flexible side group like an alkyl chain lowers  $T_g$  because a segment containing the substituent can move through a smaller unoccupied volume in the solid than one in which the pendant group has more rigid steric requirements. Larger substituents prevent efficient packing of macromolecules in the absence of crystallization, but motion of the polymer chain is freed only if the substituent itself can change its conformation readily. The interplay of these two influences is shown in Table 4.2 for the methacrylate polymers.

Stronger intermolecular attractive forces pull the chains together and hinder relative motions of segments of different macromolecules. Polar polymers and those in which hydrogen bonding or other specific interactions are important therefore have high  $T_g$ . Glass transition temperatures are in this order: polyacrylonitrile > poly(vinyl alcohol) > poly(vinyl acetate) > polypropylene.

Polymers of vinylidene monomers (1,1-disubstituted ethylenes) have lower  $T_g$ 's than the corresponding vinyl polymers. Polyisobutene and polypropylene comprise such a pair and so do poly(vinylidene chloride) and poly(vinyl chloride). Symmetrical disubstituted polymers have lower  $T_g$ 's than the monosubstituted macromolecules because no conformation is an appreciably lower energy form than any other (cf. the discussion of polyisobutene in Section 1.13).

For a given polymer type,  $T_g$  increases with number average molecular weight according to

$$T_g = T_g^\infty - u/\bar{M}_n \quad (4-4)$$

where  $T_g^\infty$  is the glass-to-rubber transition temperature of an infinitely long polymer chain and  $u$  is a constant that depends on the polymer. Observed  $T_g$ 's level off within experimental uncertainty at a degree of polymerization between 500 and 1000, for vinyl polymers. Thus  $T_g$  is 88 °C for polystyrene with  $\bar{M}_n > 10,000$  and 100 °C for the same polymer with  $\bar{M}_n > 50,000$ .

Cross-linking increases the glass transition temperature of a polymer when the average size of the segments between cross-links is the same or less than the lengths of the main chain that can start to move at temperatures near  $T_g$ . The glass transition temperature changes little with the degree of cross-linking when the crosslinks are widely spaced, as they are in normal vulcanized rubber. Large shifts of  $T_g$  with increased cross-linking are observed, however, in polymers that are already highly cross-linked, as in the "cure" of epoxy (Section 1.3.3) and phenolic (Fig. 8.1) thermosetting resins.

The glass transition temperature of miscible polymer mixtures can be calculated from

$$\frac{1}{T_g} \simeq \frac{w_A}{T_{gA}} + \frac{w_B}{T_{gB}} \quad (4-5)$$

where  $T_{gi}$  and  $w_i$  are the glass temperature (in K) and weight fraction of component  $i$  of the compound. This equation is useful with plasticizers (Section 5.3.2) which are materials that enhance the flexibility of the polymer with which they are mixed. The  $T_g$  values of plasticizers themselves are most effectively estimated by using Eq. (4-5) with two plasticized mixtures of known compositions and measured  $T_g$ 's. The foregoing equation cannot be applied to polymer blends in which the components are not mutually soluble, because each ingredient will exhibit its characteristic  $T_g$  in such mixtures. The existence of a single glass temperature is in fact a widely used criterion for miscibility in such materials (Section 5.1).

Equation (4-5) is also a useful guide to the glass transition temperatures of statistical copolymers. In that case  $T_{gA}$  and  $T_{gB}$  refer to the glass temperatures of the corresponding homopolymers. It will not apply, however, to block and graft copolymers in which a separate  $T_g$  will be observed for each component polymer if the blocks or branches are long enough to permit each homopolymer type to segregate into its own region. This separation into different domains is necessary for the use of styrene–butadiene block polymers as thermoplastic rubbers.

#### 4.4.3 Correlations between $T_m$ and $T_g$

A rough correlation exists between  $T_g$  and  $T_m$  for crystallizable polymers, although the molecular mechanisms that underlie both transitions differ. Any structural feature that enhances chain stiffness will raise  $T_g$ , since this is the temperature needed for the onset of large-scale segmental motion. Stronger intermolecular forces will also produce higher  $T_g$ 's. These same factors increase  $T_m$ , as described in Section 4.3, in connection with Eq. (4-1).

Statistical copolymers of the types described in Chapter 10 tend to have broader glass transition regions than homopolymers. The two comonomers usually do not fit into a common crystal lattice and the melting points of copolymers will be lower and their melting ranges will be broader, if they crystallize at all. Branched and linear polyethylene provide a case in point since the branched polymer can be regarded as a copolymer of ethylene and higher 1-olefins.

#### 4.4.4 Measurement of $T_g$

Glass transition temperatures can be measured by many techniques. Not all methods will yield the same value because this transition is rate dependent. Polymer segments will respond to an applied stress by flowing past each other if the

sample is deformed slowly enough to allow such movements to take place at the experimental temperature. Such deformation will not be recovered when the stress is released if the experiment has been performed above  $T_g$ . If the rate at which the specimen is deformed in a particular experiment is too fast to allow the macromolecular segments to respond by flowing, the polymer will be observed to be glassy. It will either break before the test is completed or recover its original dimensions when the stress is removed. In either event, the experimental temperature will have been indicated to be below  $T_g$ . As a consequence, observed glass transition temperatures vary directly with the rates of the experiments in which they are measured.

The  $T_g$  values quoted in Table 4.2 are either measured by very slow rate methods or are obtained by extrapolating the data from faster, nonequilibrium techniques to zero rates. This is a fairly common practice, in order that the glass transition temperature can be considered as characteristic only of the polymer and not of the measuring method.

Many relatively slow or static methods have been used to measure  $T_g$ . These include techniques for determining the density or specific volume of the polymer as a function of temperature (cf. Fig. 4.1) as well as measurements of refractive index, elastic modulus, and other properties. Differential thermal analysis and differential scanning calorimetry are widely used for this purpose at present, with simple extrapolative corrections for the effects of heating or cooling rates on the observed values of  $T_g$ . These two methods reflect the changes in specific heat of the polymer at the glass-to-rubber transition. Dynamic mechanical measurements, which are described in Sections 4.7.1 and 4.8, are also widely employed for locating  $T_g$ .

In addition, there are many related industrial measurements based on softening point, hardness, stiffness, or deflection under load while the temperature is being varied at a stipulated rate. No attempt is usually made to compensate for heating rate in these methods, which yield transition temperatures about 10–20° higher than those from the other procedures mentioned. Some technical literature that is used for design with plastics quotes brittleness temperatures rather than  $T_g$ . The former is usually that temperature at which half the specimens tested break in a specified impact test. It depends on the polymer and also on the nature of the impact, sample thickness, presence or absence of notches, and so on. Since the measured brittleness temperature is influenced very strongly by experimental conditions, it cannot be expected to correlate closely with  $T_g$  or even with the impact behavior of polymeric articles under service conditions that may differ widely from those of the brittleness test method.

Heat distortion temperatures (HDTs) are widely used as design criteria for polymeric articles. These are temperatures at which specimens with particular dimensions distort a given amount under specified loads and deformations. Various test methods, such as ASTM D648, are described in standards compilations. Because of the stress applied during the test, the HDT of a polymer is invariably higher than its  $T_g$ .

## 4.5 Rubber Elasticity

### 4.5.1 Qualitative Description of Elastomer Behavior

Unvulcanized rubber consists of a large number of flexible long molecules with a structure that permits free rotation about single bonds in the primary chain. On deformation the molecules are straightened, with a decrease in entropy. This results in a retractive force on the ends of the polymer molecules. The molecular structure of the flexible rubber molecules makes it relatively easy for them to take up statistically random conformations under thermal motion. This property is a result of the weak intermolecular attractive forces in elastomers and distinguishes them chemically from other polymers which are more suitable for use as plastics or fibers.

It is important to understand that flow and deformation in high polymers result from local motion of small segments of the polymer chain and not from concerted, instantaneous movements of the whole molecule. High elasticity results from the ability of extended polymer chains to regain a coiled shape rapidly. Flexibility of segments of the molecule is essential for this property, and this flexibility results from relative ease of rotation about the axis of the polymer chain. Figure 4.12 illustrates the mechanism of a segmental jump by rotation about two carbon–carbon bonds in a schematic chain molecule [4]. The hole in the solid structure is displaced to the right, in this scheme, as the three-carbon segment jumps to the left. Clearly, such holes (which are present in wastefully packed, i.e., noncrystalline polymers) can move through the structure.

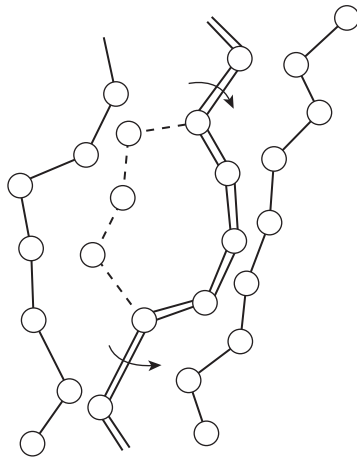


**FIGURE 4.12**

Schematic representation of a segmental jump by rotation about two carbon–carbon bonds in a macromolecular chain [4].

If molecules are restrained by entanglement with other chains or by actual chemical bonds (cross-links) between chains, deformation is still possible because of cooperative motions of local segments. This presupposes that the number of chain atoms between such restraints is very much larger than the average size of segments involved in local motions. Ordinary vulcanized natural rubber contains 0.5–5 parts (by weight) of combined sulfur vulcanizing agent per 100 parts of rubber. Approximately one of every few hundred monomer residues is cross-linked in a typical rubber with good properties (the molecular weight of the chain regions between cross-links is 20,000–25,000 in such a hydrocarbon rubber). If the cross-link density is increased, for example, by combining 30–50 parts of sulfur per 100 parts rubber, segmental motion is severely restricted. The product is a hard, rigid nonelastomeric product known as “ebonite” or “hard rubber.”

High elasticity is attributed to a shortening of the distance between the ends of chain molecules undergoing sufficient thermal agitation to produce rotations about single bonds along the main chains of the molecules. The rapid response to application and removal of stress which is characteristic of rubbery substances requires that these rotations take place with high frequency at the usage temperatures.

Rotations about single bonds are never completely free, and energy barriers that are encountered as substituents on adjacent chain atoms are turned away from staggered conformations (Fig. 1.6). These energy barriers are smallest for molecules without bulky or highly polar side groups. Unbranched and relatively symmetrical chains are apt to crystallize on orientation or cooling, however, and this is undesirable for high elasticity because the crystallites hold their constituent chains fixed in the lattice. Some degree of chain irregularity caused by copolymerization can be used to reduce the tendency to crystallize. If there are double bonds in the polymer chain as in 1,4-polydienes like natural rubber, the *cis* configuration produces a lower packing density; there is more free space available for segmental jumps and the more irregular arrangement reduces the ease of crystallization. Thus *cis*-polyisoprene (natural rubber) is a useful elastomer while *trans*-polyisoprene is not.

The molecular requirements of elastomers can be summarized as follows:

1. The material must be a high polymer.
2. Its molecules must remain flexible at all usage temperatures.
3. It must be amorphous in its unstressed state. (Polyethylene is not an elastomer, but copolymerization of ethylene with sufficient propylene reduces chain regularity sufficiently to eliminate crystallinity and produce a useful elastomer.)
4. For a polymer to be useful as an elastomer, it must be possible to introduce cross-links in such a way as to bond a macroscopic sample into a continuous network. Generally, this requires the presence of double bonds or chemically functional groups along the chain.

Polymers that are not cross-linked to form infinite networks can behave elastically under transient stressing conditions. They cannot sustain prolonged loads,

however, because the molecules can flow past each other to relieve the stress, and the shape of the article will be deformed by this creep process. (Alternatives to cross-linking are mentioned in Sections 1.5.4 and 11.2.6)

Polybutadiene with no substituent groups larger than hydrogen has greater resilience than natural rubber, in which a methyl group is contained in each isoprene repeating unit. Polychloroprenes (neoprenes) have superior oil resistance but lose their elasticity more readily at low temperatures since the substituent is a bulky, polar chlorine atom. (The structures of these monomers are given in Fig. 1.4.)

### 4.5.2 Rubber as an Entropy Spring

*Disorder makes nothing at all, but unmakes everything.*

—John Stuart Blackie

Bond rotations and segmental jumps occur in a piece of rubber at high speed at room temperature. A segmental movement changes the overall conformation of the molecule. There will be a very great number of equi-energetic conformations available to a long chain molecule. Most of these will involve compact rather than extended contours. There are billions of compact conformations but only one fully extended one. Thus, when the ends of the molecule are far apart because of uncoiling in response to an applied force, bond rotations after release of the force will turn the molecule into a compact, more shortened state just by chance. About 1000 individual C—C bonds in a typical hydrocarbon elastomer must change conformation when a sample of fully extended material retracts to its shortest state at room temperature [5]. There need not be any energy changes involved in this change. It arises simply because of the very high probability of compact compared to extended conformations.

An elastomer is essentially an *entropy spring*. This is in contrast to a steel wire, which is an *energy spring*. When the steel spring is distorted, its constituent atoms are displaced from their equilibrium lowest energy positions. Release of the applied force causes a retraction because of the net gain in energy on recovering the original shape. An energy spring warms on retraction. An ideal energy spring is a crystalline solid with Young's modulus about  $10^{11}$ – $10^{12}$  dyn/cm ( $10^{10}$ – $10^{11}$  N/m<sup>2</sup>). It has a very small ultimate elongation. The force required to hold the energy spring at constant length is inversely proportional to temperature. In thermodynamic terms  $(\partial U/\partial l)_T$  is large and positive, where  $U$  is the internal energy thermodynamic state function.

An ideal elastomer has Young's modulus about  $10^6$ – $10^7$  dyn/cm<sup>2</sup> ( $10^5$ – $10^6$  N/m<sup>2</sup>) and reversible elasticity of hundreds of percent elongation. The force required to hold this entropy spring at fixed length falls as the temperature is lowered. This implies that  $(\partial U/\partial l)_T = 0$ .

#### 4.5.2.1 Ideal Elastomer and Ideal Gas

An ideal gas and an ideal elastomer are both entropy springs.

The molecules of an ideal gas are independent agents. By definition, there is no intermolecular attraction. The pressure of the gas on the walls of its container

is due to random thermal bombardment of the molecules on the walls. The tension of rubber against restraining clamps is due to random coiling and uncoiling of chain molecules. The molecules of an ideal elastomer are independent agents. There is no intermolecular attraction, by definition. (If there is appreciable intermolecular attraction, the material will not exhibit high elasticity, as we saw earlier.)

Gas molecules tend to their most likely distribution in space. The molecules of an ideal elastomer tend to their most probable conformation, which is that of a random coil. The most probable state in either case is that in which the entropy is a maximum.

If the temperature of an ideal gas is increased at constant volume, its pressure rises in direct proportion to the temperature. Similarly, the tension of a rubber specimen at constant elongation is directly proportional to temperature. An ideal gas undergoes no temperature change on expanding into a vacuum. An ideal rubber retracting without load at constant volume undergoes no temperature change. Under adiabatic conditions, an ideal gas cools during expansion against an opposing piston, and a stretched rubber cools during retraction against a load.

Table 4.3 lists the thermodynamic relations between pressure, volume, and temperature of an ideal gas and its internal energy  $U$  and entropy  $S$ . We see that the definition of an ideal gas leads to the conclusion that the pressure exerted by such a material is entirely due to an entropy contribution. If an ideal gas confined at a certain pressure were allowed to expand against a lower pressure, the increase in volume would result in the gas going to a state of greater entropy. The internal energy of the ideal gas is not changed in expanding at constant temperature.

#### 4.5.2.2 Thermodynamics of Rubber Elasticity

In an ideal gas we considered the relations between the thermodynamic properties  $S$  and  $U$ , on the other hand, and the state variables  $P$ ,  $V$ , and  $T$  of the substance. With an ideal elastomer we shall be concerned with the relation between  $U$  and  $S$  and the state variables force, length, and temperature.

The first law of thermodynamics defines the internal energy from

$$dU \equiv dq + dw \quad (4-6)$$

(The increased  $dU$  in any change taking place in a system equals the sum of the energy added to the system by the heat process,  $dq$ , and the work performed on it,  $dw$ .)

The second law of thermodynamics defines the entropy change  $dS$  in any reversible process:

$$T dS = dq_{\text{rev}} \quad (4-7)$$

**Table 4.3** Ideal Gas as an Entropy Spring,

First and second laws of thermodynamics applied to compression of a gas:

$$dU = dq + dw \quad (\text{i})$$

where  $U$  = internal energy function,  $dq$  = heat absorbed by substance, and  $dw$  = work done on substance by its surroundings.

$$dU = T dS - P dV \quad (\text{ii})$$

Equation (ii) yields

$$P = T(\partial S/\partial V)_T - (\partial U/\partial V)_T = -(\partial A/\partial V)_T \quad (\text{iii})$$

where  $S$  = entropy and  $A$  = Helmholtz free energy  $\equiv U - TS$ .

From (iii), the pressure consists of two terms:

entropy contribution:  $T(\partial S/\partial V)_T$  (called kinetic pressure)

internal energy contribution:  $-(\partial U/\partial V)_T$  (called internal pressure)

To evaluate the terms in Eq. (iii) experimentally, substitute

entropy contribution:  $T(\partial S/\partial V)_T = T(\partial P/\partial T)_V$

Thus,

$$P = T(\partial P/\partial T)_V - (\partial U/\partial V)_T \quad (\text{iiia})$$

internal energy contribution to the total pressure:

$$P - T(\partial P/\partial T)_V \quad (\text{iv})$$

Definition of *ideal gas* is gas which obeys the equation of state:

$$PV = nRT$$

and for which the internal energy  $U$  is a function of temperature only, i.e.,

$$(\partial U/\partial V)_T = (\partial U/\partial P)_T = 0 \quad (\text{ideal gas}) \quad (\text{vi})$$

It follows that

$$P = T(\partial P/\partial T)_V \quad (\text{ideal gas}) \quad (\text{vii})$$

and the pressure is due only to the entropy contribution.

(A reversible process is the thermodynamic analog of frictionless motion in mechanics. When a process has been conducted reversibly, we can, by performing the inverse process in reverse, set the system back in precisely its initial state, with zero net expenditure of work in the overall process. The system and its surroundings are once again exactly as they were at the beginning. A reversible process is an idealization which constitutes a limit that may be approached but not attained in real processes.)

For a reversible process, Eqs. (4-6) and (4-7) yield

$$dU = T dS + dw \quad (4-8)$$

We define the Helmholtz free energy  $A$  as

$$A \equiv U - TS \quad (4-9)$$

(This is a useful thermodynamic quantity to characterize changes at constant volume of the working substance.) For a change at constant temperature, from Eq. (4-26),

$$dA = dU - T dS \quad (4-10)$$

Combining Eqs. (4-25) and (4-26)

$$dA = dw \quad (4-11)$$

That is, the change in  $A$  in an isothermal process equals the work done on the system by its surroundings. Conventionally, when gases and liquids are of major interest the work done on the system is written  $dw = -P dV$ . When we consider elastic solids, the work done by the stress is important. If tensile force is  $f$  and  $l$  is the initial length of the elastic specimen in the direction of the force, the work done in creating an elongation  $dl$  is

$$dw = f dl \quad (4-12)$$

If a hydrostatic pressure  $P$  is acting in addition to the tensile force  $f$ , the total work on the system is

$$dw = f dl - P dV \quad (4-13)$$

In the case of rubbers,  $dV$  is very small and if  $P = 1$  atm,  $P dV$  is less than  $10^{-3} f dl$ . Thus we can neglect  $P dV$  and use Eq. (4-12).

From Eqs. (4-11) and (4-12),

$$(\partial A / \partial l)_T = (\partial w / \partial l)_T = f \quad (4-14)$$

That is, the tension is equal to the change in Helmholtz free energy per unit extension. From Eqs. (4-10) and (4-12),

$$(\partial A / \partial l)_T = (\partial U / \partial l)_T - (\partial S / \partial l)_T = f \quad (4-15)$$

Thus, the force consists of an internal energy component and an entropy component [compare (iii) of Table 4.1 for the pressure of a gas].

To evaluate Eq. (4-15) experimentally, we proceed in an analogous fashion to the method used to estimate the entropy component of the pressure of a gas (Table 4.3). From Eq. (4-9), for any change,

$$dA = dU - T dS - S dT \quad (4-16)$$

For a reversible change, from Eqs. (4-8) and (4-12),

$$dU = f dl + T dS \quad (4-17)$$

Combining the last two equations,

$$dA = f dl - S dT \quad (4-18)$$

Thus, by partial differentiation,

$$(\partial A / \partial l)_T = f$$

$$(\partial A / \partial T)_l = -S \quad (4-19)$$

Since

$$\frac{\partial}{\partial l} \left( \frac{\partial A}{\partial T} \right)_l = \frac{\partial}{\partial T} \left( \frac{\partial A}{\partial l} \right)_T \quad (4-20)$$

we can substitute Eqs. (4-14) and (4-19) into Eq. (4-20) to obtain

$$(\partial S / \partial l)_T = -(\partial f / \partial T)_l \quad (4-21)$$

This gives the entropy change per unit extension,  $(\partial S / \partial l)_T$ , which occurs in Eq. (4-15), in terms of the temperature coefficient of tension at constant length  $(\partial f / \partial T)_l$ , which can be measured. With Eq. (4-21), Eq. (4-15) becomes

$$(\partial U / \partial l)_T = f - T(\partial f / \partial T)_l \quad (4-22)$$

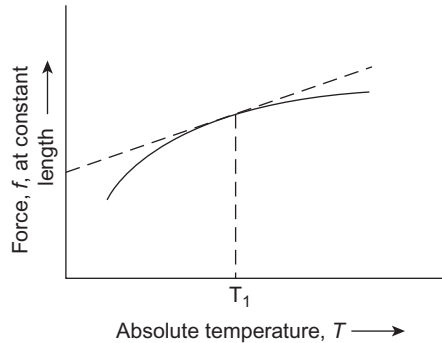
where  $(\partial U / \partial l)_T$  is the internal energy contribution to the total force. [Compare Eq. (iv) in Table 4.3 for a gas.]

Figure 4.13 shows how experimental data can be used with Eqs. (4-21) and (4-22) to determine the internal energy and entropy changes accompanying deformation of an elastomer. Such experiments are simple in principle but difficult in practice because it is hard to obtain equilibrium values of stress.

For an ideal elastomer  $(\partial U / \partial l)_T$  is zero and Eq. (4-22) reduces to

$$f = T(\partial f / \partial T)_l \quad (4-23)$$

in complete analogy to Eq. (vii) of Table 4.3 for an ideal gas. In real elastomers, chain uncoiling must involve the surmounting of bond rotational energy barriers



**FIGURE 4.13**

Experimental measurement of  $(\partial f / \partial l)_T$  and  $(\partial U / \partial l)_T$ . The slope of the tangent to the curve at temperature  $T_1 = (\partial f / \partial T)_l$  at  $T_1$ . This equals  $(\partial S / \partial l)_T$ , which equals entropy change per unit extension when the elastomer is extended isothermally at  $T_1$ . The intercept on the force axis equals  $(\partial U / \partial l)_T$  since this corresponds to  $T = 0$  in Eq. (4-22). The intercept is the internal energy change per unit extension.

but this means that the internal energy term  $(\partial U/\partial l)_T$  cannot be identically zero, however.

If the internal energy contribution to the force at constant length and sample volume is  $f_e$ , its relative contribution is

$$\frac{f_e}{f} = 1 - \frac{T}{f} \left( \frac{\partial f}{\partial T} \right)_{v,l} \quad (4-24)$$

Various measurements have shown that  $f_e/f$  is about 0.1-0.2 for polybutadiene and *cis*-polyisoprene elastomers. These polymers are essentially but not entirely entropy springs.

#### 4.5.2.3 Stress–Strain Properties of Cross-Linked Elastomers

Consider a cube of cross-linked elastomer with unit dimensions. This specimen is subjected to a tensile force  $f$ . The ratio of the increase in length to the unstretched length is the nominal strain  $\varepsilon$  (epsilon), but the deformation is sometimes also expressed as the extension ratio  $\Lambda$  (lambda):

$$\Lambda = \lambda/\lambda_0 = 1 + \varepsilon \quad (4-25)$$

where  $\lambda$  and  $\lambda_0$  are the stretched and unstretched specimen lengths, respectively. With a cube of unit initial dimensions, the stress  $\tau$  is equal to  $f$ . (Recall the definitions of stress, normal strain, and modulus on page 24.) Also, in this special case  $d\lambda = \lambda_0 d\Lambda = d\Lambda$ , and so Eqs. (4-21) and (4-23) are equivalent to

$$\tau = -T(\partial S/\partial \Lambda)_{T,V} \quad (4-26)$$

Statistical mechanical calculations [6] have shown that the entropy change is given by

$$\Delta S = -\frac{1}{2}N\kappa(\Lambda^2 + (2/\Lambda) - 3) \quad (4-27)$$

where  $N$  is the number of chain segments between cross-links per unit volume and  $\kappa$  (kappa) is Boltzmann's constant ( $R/L$ ). Then, from Eq. (4-26),

$$\tau = N\kappa T(\Lambda - 1/\Lambda^2) \quad (4-28)$$

Equation (4-28) is equivalent to

$$\tau = (\rho RT/M_c)(\Lambda - 1/\Lambda^2) \quad (4-29)$$

where  $\rho$  is the elastomer density (gram per unit volume),  $M_c$  is the average molecular weight between cross-links ( $M_c = \rho L/N$ ), and  $L$  is Avogadro's constant.

Equation (4-29) predicts that the stress–strain properties of an elastomer that behaves like an entropy spring will depend only on the temperature, the density

of the material, and the average molecular weight between cross-links. In terms of nominal strain this equation is approximately

$$\tau = (\rho RT/M_c)(3\varepsilon + 3\varepsilon^2 + \dots) \quad (4-30)$$

and at low strains, Young's modulus,  $Y$ , is

$$Y \equiv d\tau/d\varepsilon = 3\rho RT/M_c \quad (4-31)$$

The more tightly cross-linked the elastomer, the lower will be  $M_c$  and the higher will be its modulus. That is, it will take more force to extend the polymer a given amount at fixed temperature. Also, because the elastomer is an entropy spring, the modulus will increase with temperature.

Equation (4-29) is valid for small extensions only. The actual behavior of real cross-linked elastomers in uniaxial extension is described by the Mooney–Rivlin equation which is similar in form to Eq. (4-29):

$$\tau = (C_1 + C_2/\Lambda)(\Lambda - 1/\Lambda^2) \quad (4-32)$$

Here  $C_1$  and  $C_2$  are empirical constants, and  $C_1$  is often assumed to be equal to  $\rho RT/M_c$ .

#### EXAMPLE 4-1

Given an SBR rubber (23.5 mol% styrene) that has an  $M_n$  of 100,000 before cross-linking. Calculate the engineering stress in the units of  $MN/m^2$  at 100% elongation of the cross-linked elastomer with an  $M_c$  of 10,000 at 25 °C. Also calculate the corresponding modulus at very low extensions. The density of the cross-linked elastomer is 0.98  $g/cm^3$ .

A 100% elongation means that  $\Lambda = 2\lambda_0/\lambda = 2$ .  $\tau$  and  $Y$  can be calculated using Eqs. (4-29) and (4-31), respectively.

$$\tau = \frac{0.98 \times 10^6 \times 8.3143 \times 298}{10,000} \left(2 - \frac{1}{4}\right) = 425,000 \frac{N}{m^2} = 0.425 \frac{MN}{m^2}$$

$$Y = \frac{3 \times 0.98 \times 10^6 \times 8.3143 \times 298}{10,000} = 728,000 \frac{N}{m^2} = 0.728 \frac{MN}{m^2}$$

#### 4.5.2.4 Real and Ideal Rubbers

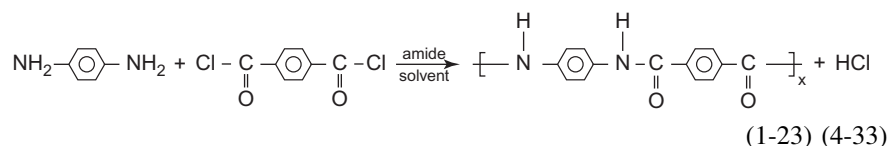
To this point, we have emphasized that the retractive force in a stretched ideal elastomer is directly proportional to its temperature. In a cross-linked, real elastomer that has been reinforced with carbon black, as is the usual practice, the force to produce a given elongation may actually be seen to *decrease* with increased temperature. This is because the anchor regions that hold the elastomer chains together are not only chemical cross-links, as assumed in the ideal theory. They also comprise physical entanglements of polymer molecules and rubber-carbon

black adsorption sites. Entanglements will be more labile at higher temperatures, where the molecular chains are more flexible, with a net decrease in the number of effective intermolecular anchor points, an increase in  $M_c$ , and a decrease in the retractive force, according to Eq. (4-31).

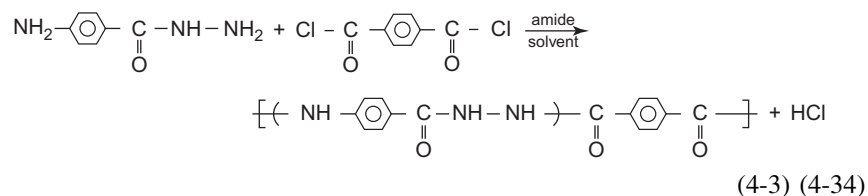
## 4.6 Rodlike Macromolecules

Very rigid macromolecules are at the opposite end of the spectrum of properties from elastomers, which are characterized by weak intermolecular forces, a high degree of molecular flexibility, and an absence of regular intermolecular order.

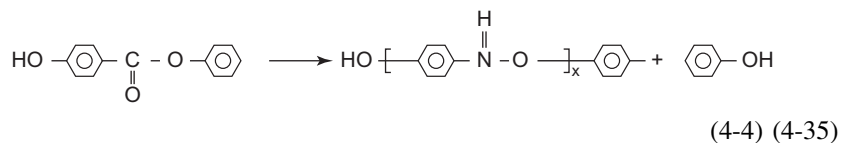
Aromatic polyamides and polyesters are examples of stiff chain polymers. Poly(*p*-phenylene terephthalamide) (Kevlar™, 1-23) can be made by reaction (4-33) in a mixture of hexamethylphosphoramide and *N*-methylpyrrolidone:



Polyamide-hydrazides



and aromatic polyesters like poly(*p*-hydroxybenzoic acid)



also provide rodlike species. These polymers behave in solution like logs on a pond rather than like random coils. They exhibit liquid crystalline properties where they have the short-range order of nematic mesophases. The liquid crystals are readily oriented under shear and can be used to produce very highly oriented ultrastrong fibers. On a specific weight basis they are stronger and stiffer than steel or glass and are used to reinforce flexible and rigid composites like tires, conveyor belts, and body armor as well as to make industrial and military protective clothing.

## 4.7 Polymer Viscoelasticity

An ideal elastic material is one that exhibits no time effects. When a stress  $\sigma$  is applied the body deforms immediately to a strain  $e$ . (These terms were defined broadly in Section 1.8.) The sample recovers its original dimensions completely and instantaneously when the stress is removed. Further, the strain is always proportional to the stress and is independent of the rate at which the body is deformed:

$$\sigma = Y\varepsilon \quad (4-36)$$

where  $Y$  is Young's modulus if the deformation mode is a tensile stretch and Eq. (4-36) is an expression of the familiar Hooke's law. The changes in the shape of an isotropic, perfectly elastic material will always be proportional to the magnitude of the applied stress if the body is twisted, sheared, or compressed instead of extended, but the particular stress/strain (modulus) will differ from  $Y$ . Figure 4.14 summarizes the concepts and symbols for the elastic constants in tensile, shear, and bulk deformations.

An experiment such as that in Fig. 4.14a can produce changes in the volume as well as the shape of the test specimen. The elastic moduli listed in this figure are related by Poisson's ratio  $\beta$ , which is a measure of the lateral contraction accompanying a longitudinal extension:

$$\beta = \frac{1}{2} [1 - (1/V)\partial V/\partial\varepsilon] \quad (4-37)$$

where  $V$  is the volume of the sample. When there is no significant volume change,  $\partial V/\partial\varepsilon = 0$  and  $\beta = 0.5$ . This behavior is characteristic of ideal rubbers. Real solids dilate when extended, and values of  $\beta$  down to about 0.2 are observed for rigid, brittle materials. The moduli in the elastic behavior of isotropic solids are related by

$$Y = 2G(1 + \beta) = 3K(1 - 2\beta) \quad (4-38)$$

At very low extensions when there is no significant amount of permanent deformation  $Y/G$  is between about 2.5 for rigid solids and 3 for elastomeric materials.

An ideal Newtonian fluid was described in Section 4.13. Such a material has no elastic character; it cannot support a strain and the instantaneous response to a shearing stress  $\tau$  is viscous flow:

$$\tau = \eta\dot{\gamma} \quad (4-39)$$

Here  $\dot{\gamma}$  is the shear rate or velocity gradient ( $= d\gamma/dt$ ) and  $\eta$  is the viscosity which was first defined in Section 3.3.

Polymeric (and other) solids and liquids are intermediate in behavior between Hookean, elastic solids, and Newtonian purely viscous fluids. They often exhibit elements of both types of responses, depending on the time scale of the experiment. Application of stresses for relatively long times may cause some flow and

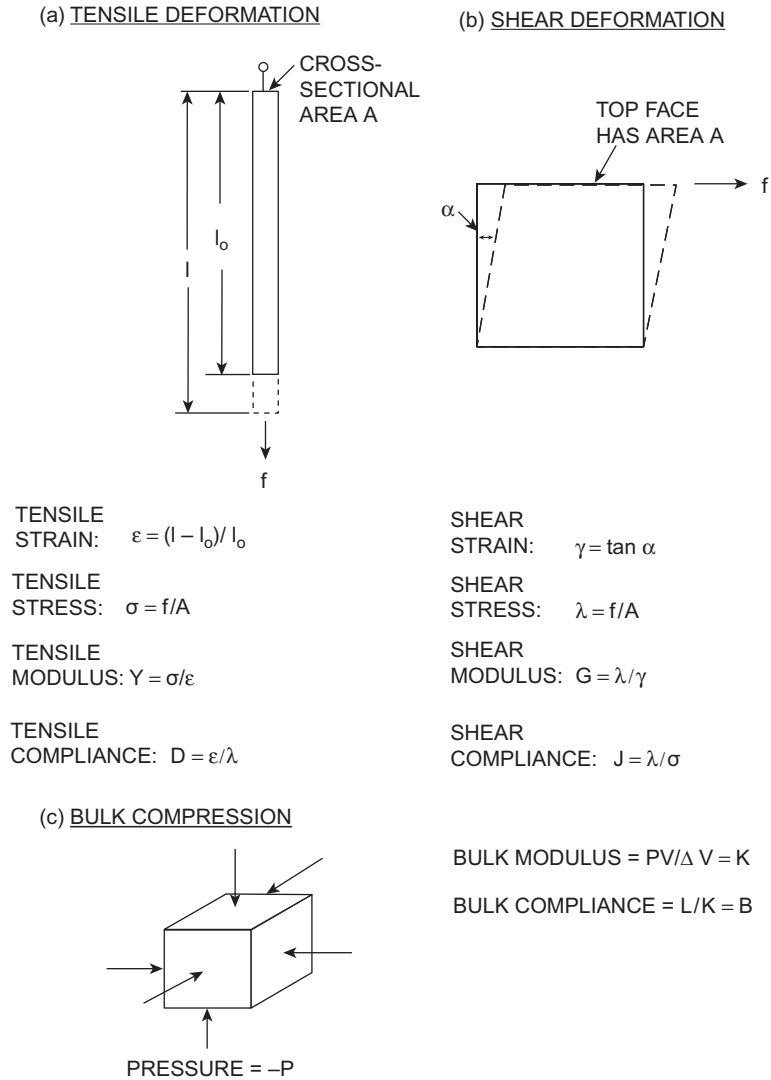


**FIGURE 4.14**

(a) Elastic constants in tensile deformation. (b) Elastic constants in shear deformation. (c) Elastic constants in volume deformation.

permanent deformation in solid polymers while rapid shearing will induce elastic behavior in some macromolecular liquids. It is also frequently observed that the value of a measured modulus or viscosity is time dependent and reflects the manner in which the measuring experiment was performed. These phenomena are examples of *viscoelastic* behavior.

Three types of experiments are used in the study of viscoelasticity. These involve creep, stress relaxation, and dynamic techniques. In creep studies a body is subjected to a constant stress and the sample dimensions are monitored as a function of time. When the polymer is first loaded an immediate deformation occurs, followed by progressively slower dimensional changes as the sample creeps toward a limiting shape. Figure 1.3 shows examples of the different behaviors observed in such experiments.

Stress relaxation is an alternative procedure. Here an instantaneous, fixed deformation is imposed on a sample, and the stress decay is followed with time. A very useful modification of these two basic techniques involves the use of a periodically varying stress or deformation instead of a constant load or strain. The dynamic responses of the body are measured under such conditions.

#### 4.7.1 Phenomenological Viscoelasticity

Consider the tensile experiment of Fig. 4.14a as a creep study in which a steady stress  $\tau_0$  is suddenly applied to the polymer specimen. In general, the resulting strain  $\varepsilon(t)$  will be a function of time starting from the imposition of the load. The results of creep experiments are often expressed in terms of compliances rather than moduli. The tensile creep compliance  $D(t)$  is

$$D(t) = \varepsilon(t)/\sigma_0 \quad (4-40)$$

The shear creep compliance  $J(t)$  (see Fig. 4.14b) is similarly defined as

$$J(t) = \gamma(t)/\tau_0 \quad (4-41)$$

where  $\varepsilon_0$  is the constant shear stress and  $\gamma(t)$  is the resulting time-dependent strain.

Stress relaxation experiments correspond to the situations in which the deformations sketched in Fig. 4.14 are imposed suddenly and held fixed while the resulting stresses are followed with time. The tensile relaxation modulus  $Y(t)$  is then obtained as

$$Y(t) = \sigma(t)/\varepsilon_0 \quad (4-42)$$

with  $\varepsilon_0$  being the constant strain. Similarly, a shear relaxation experiment measures the shear relaxation modulus  $G(t)$ :

$$G(t) = \tau(t)/\gamma_0 \quad (4-43)$$

where  $\gamma_0$  is the constant strain.

Although a compliance is the inverse of a modulus for an ideal elastic body, this is not true for viscoelastic materials. That is,

$$Y(t) = \sigma(t)/\varepsilon_0 \neq \varepsilon(t)/\sigma_0 = D(t) \quad (4-44)$$

and

$$G(t) = \tau(t)/\gamma_0 \neq \gamma(t)/\tau_0 = J(t) \quad (4-45)$$

Consider two experiments carried out with identical samples of a viscoelastic material. In experiment (a) the sample is subjected to a stress  $\sigma_1$  for a time  $t$ . The resulting strain at  $t$  is  $\varepsilon_1$ , and the creep compliance measured at that time is  $D_1(t) = \varepsilon_1/\sigma_1$ . In experiment (b) a sample is stressed to a level  $\sigma_2$  such that strain  $\varepsilon_1$  is achieved immediately. The stress is then gradually decreased so that the strain remains at  $\varepsilon_1$  for time  $t$  (i.e., the sample does not creep further). The stress on the material at time  $t$  will be  $\sigma_3$ , and the corresponding relaxation modulus will be  $Y_2(t) = \sigma_3/\varepsilon_1$ . In measurements of this type, it can be expected that  $\sigma_2 > \sigma_1 > \sigma_3$  and  $Y(t) \neq (D(t))^{-1}$ , as indicated in Eq. (4-44).  $G(t)$  and  $Y(t)$  are obtained directly only from stress relaxation measurements, while  $D(t)$  and  $J(t)$  require creep experiments for their direct observation. These various parameters can be related in the linear viscoelastic region described in Section 4.7.2.

#### 4.7.1.1 Terminology of Dynamic Mechanical Experiments

A complete description of the viscoelastic properties of a material requires information over very long times. Creep and stress relaxation measurements are limited by inertial and experimental limitations at short times and by the patience of the investigator and structural changes in the test material at very long times. To supplement these methods, the stress or the strain can be varied sinusoidally in a dynamic mechanical experiment. The frequency of this alternation is  $\nu$  cycles/sec or  $\omega (= 2\pi\nu)$  rad/sec. An alternating experiment at frequency  $\omega$  is qualitatively equivalent to a creep or stress relaxation measurement at a time  $t = (1/\omega)$  sec.

In a dynamic experiment, the stress will be directly proportional to the strain if the magnitude of the strain is small enough. Then, if the stress is applied sinusoidally the resulting strain will also vary sinusoidally. In special cases the stress and the strain will be in phase. A cross-linked amorphous polymer, for example, will behave elastically at sufficiently high frequencies. This is the situation depicted in Fig. 4.15a where the stress and strain are in phase and the strain is small. At sufficiently low frequencies, the strain will be  $90^\circ$  out of phase with the stress as shown in Fig. 4.15c. In the general case, however, stress and strain will be out of phase (Fig. 4.15b).

In the last instance, the stress can be factored into two components, one of which is in phase with the strain and the other of which leads the strain by  $\pi/2$  rad. (Alternatively, the strain could be decomposed into a component in phase with the stress and one which lagged behind the stress by  $90^\circ$ .) This is accomplished by use of a rotating vector scheme, as shown in Fig. 4.16. The magnitude of the stress at any time is represented by the projection  $OC$  of the vector  $\mathbf{OA}$  on the vertical axis. Vector  $\mathbf{OA}$  rotates counterclockwise in this representation with a frequency  $\omega$  equal to that of the sinusoidally varying stress. The length of  $\mathbf{OA}$  is the stress amplitude (maximum stress) involved in the experiment. The strain is represented by the projection  $OD$  of vector  $\mathbf{OB}$  on the vertical axis. The strain

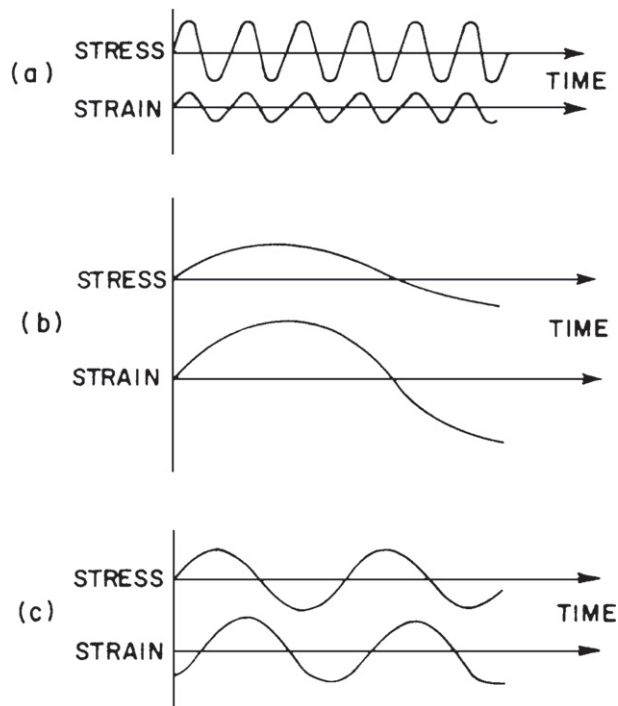


**FIGURE 4.15**

Effect of frequency on dynamic response of an amorphous, lightly cross-linked polymer: (a) elastic behavior at high frequency—stress and strain are in phase, (b) liquid-like behavior at low frequency—stress and strain are  $90^\circ$  out of phase, and (c) general case—stress and strain are out of phase.

vector **OB** also rotates counterclockwise with frequency  $\omega$  but it lags **OA** by an angle  $\delta$ . The *loss tangent* is defined as  $\tan \delta$ .

The strain vector **OB** can be resolved into vector **OE** along the direction of **OA** and **OF** perpendicular to **OA**. Then the projection **OH** of **OE** on the vertical axis is the magnitude of the strain, which is in phase with the stress at any time. Similarly, projection **OI** of vector **OF** is the magnitude of the strain, which is  $90^\circ$  (one-quarter cycle) out of phase with the stress. The stress can be similarly resolved into two components with one along the direction of **OB** and one leading the strain vector by  $\pi/2$  rad.

When the stress is decomposed into two components the ratio of the in-phase stress to the strain amplitude ( $\gamma_a$ , maximum strain) is called the *storage modulus*. This quantity is labeled  $G'(\omega)$  in a shear deformation experiment. The ratio of the out-of-phase stress to the strain amplitude is the *loss modulus*  $G''(\omega)$ . Alternatively, if the strain vector is resolved into its components, the ratio of the

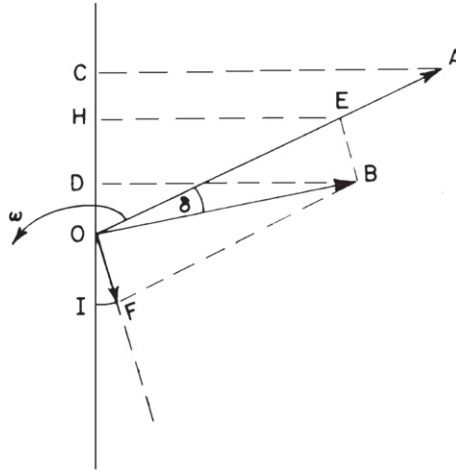


FIGURE 4.16

Decomposition of strain vector into two components in a dynamic experiment.

in-phase strain to the stress amplitude  $\tau_a$  is the storage compliance  $J'(\omega)$ , and the ratio of the out-of-phase strain to the stress amplitude is the loss compliance  $J''(\omega)$ .  $G'(\omega)$  and  $J'(\omega)$  are associated with the periodic storage and complete release of energy in the sinusoidal deformation process. The loss parameters  $G''(\omega)$  and  $J''(\omega)$  on the other hand reflect the nonrecoverable use of applied mechanical energy to cause flow in the specimen. At a specified frequency and temperature, the dynamic response of a polymer can be summarized by any one of the following pairs of parameters:  $G'(\omega)$  and  $G''(\omega)$ ,  $J'(\omega)$  and  $J''(\omega)$ , or  $\tau_a/\gamma_a$  (the absolute modulus  $|G|$ ) and  $\tan \delta$ .

An alternative set of terms is best introduced by noting that a complex number can be represented as in Fig. 4.17 by a point  $P$  (with coordinates  $x$  and  $y$ ) or by a vector  $\mathbf{OP}$  in a plane. Since dynamic mechanical behavior can be represented by a rotating vector in Fig. 4.15, this vector and hence the dynamic mechanical response is equivalent to a single complex quantity such as  $G^*$  (complex modulus) or  $J^*$  (complex compliance). Thus, in shear deformation,

$$G^*(\omega) = G'(\omega) + iG''(\omega) \quad (4-46)$$

$$J^*(\omega) = \frac{1}{G^*(\omega)} = \frac{1}{G'(\omega) + iG''(\omega)} = J'(\omega) - iJ''(\omega) \quad (4-47)$$

[Equation (4-47) can be derived from Eq. (4-46) by comparing the expressions for  $z$  and  $z^{-1}$  in Fig. 4.17.] It will also be apparent that

$$|G^*| = [(G')^2 + (G'')^2]^{1/2} \quad (4-48)$$

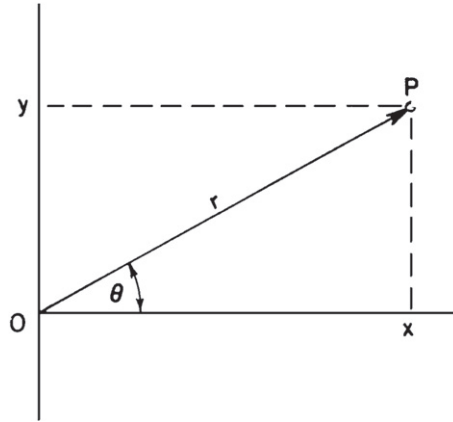


**FIGURE 4.17**

Representation of a complex number  $z = x + iy$  by a vector on the  $xy$  plane ( $i = \sqrt{-1}$ ).  
 $z = x + iy = re^{i\theta} = r(\cos \theta + i \sin \theta)$ ;  $r = |z| = |x + iy| = (x^2 + y^2)^{1/2}$ ;  $1/z = e^{-i\theta}/r = (1/r)(\cos \theta - i \sin \theta)$ .

and

$$\tan \delta = G''(\omega)/G'(\omega) = J''(\omega)/J'(\omega) \quad (4-49)$$

The real and imaginary parts of the complex numbers used here have no physical significance. This is simply a convenient way to represent the component vectors of stress and strain in a dynamic mechanical experiment.

Tan  $\delta$  measures the ratio of the work dissipated as heat to the maximum energy stored in the specimen during one cycle of a periodic deformation. The conversion of applied work to thermal energy in the sample is called *damping*. It occurs because of flow of macromolecular segments past each other in the sample. The energy dissipated per cycle due to such viscoelastic losses is  $\pi\gamma_a^2 G''$ .

For low strains and damping the dynamic modulus  $G'$  will have the same magnitude as that obtained from other methods like stress relaxation or tensile tests, provided the time scales are similar in these experiments.

Viscosity is the ratio of a stress to a strain rate [Eq. (4-39)]. Since the complex modulus  $G^*$  has the units of stress, it is possible to define a complex viscosity  $\eta^*$  as the ratio of  $G^*$  to a complex rate of strain:

$$\eta^*(\omega) = \frac{G^*(\omega)}{i\omega} = \frac{G'(\omega) + iG''(\omega)}{i\omega} = \eta'(\omega) - i\eta''(\omega) \quad (4-50)$$

Then it follows that

$$\eta'(\omega) = G''(\omega)/\omega \quad (4-51)$$

and

$$\eta''(\omega) = G'(\omega)/\omega \quad (4-52)$$

The  $\eta'(\omega)$  term is often called the *dynamic viscosity*. It is an energetic dissipation term related to  $G''(\omega)$  and has a value approaching that of the steady flow viscosity  $\eta$  in very low frequency measurements on polymers that are not cross-linked.

### 4.7.2 Linear Viscoelasticity

In linear viscoelastic behavior the stress and strain both vary sinusoidally, although they may not be in phase with each other. Also, the stress amplitude is linearly proportional to the strain amplitude at given temperature and frequency. Then mechanical responses observed under different test conditions can be inter-related readily. The behavior of a material in one condition can be predicted from measurement made under different circumstances.

Linear viscoelastic behavior is actually observed with polymers only in very restricted circumstances involving homogeneous, isotropic, amorphous specimens subjected to small strains at temperatures near or above  $T_g$  and under test conditions that are far removed from those in which the sample may be broken. Linear viscoelasticity theory is of limited use in predicting the service behavior of polymeric articles, because such applications often involve large strains, anisotropic objects, fracture phenomena, and other effects that result in nonlinear behavior. The theory is nevertheless valuable as a reference frame for a wide range of applications, just as the thermodynamic equations for ideal solutions help organize the observed behavior of real solutions.

The major features of linear viscoelastic behavior that will be reviewed here are the superposition principle and time–temperature equivalence. Where they are valid, both make it possible to calculate the mechanical response of a material under a wide range of conditions from a limited store of experimental information.

#### 4.7.2.1 Boltzmann Superposition Principle

The Boltzmann principle states that the effects of mechanical history of a sample are linearly additive. This applies when the stress depends on the strain or rate of strain or, alternatively, where the strain is considered a function of the stress or rate of change of stress.

In a tensile test, for example, Eq. (4-40) relates the strain and stress in a creep experiment when the stress  $\tau_0$  is applied instantaneously at time zero. If this loading were followed by application of a stress  $\sigma_1$  at time  $u_1$ , then the time-dependent strain resulting from this event alone would be

$$\varepsilon(t) = \sigma_1 D(t - u_1) \quad (4-53)$$

The total strain from the imposition of stress  $\sigma_0$  at  $t = 0$  and  $\sigma_1$  at  $t = u_1$  is

$$\varepsilon(t) = \sigma_0 D(t) + \sigma_1 D(t - u_1) \quad (4-54)$$

In general, for an experiment in which stresses  $\sigma_0, \sigma_1, \sigma_2, \dots, \sigma_n$  were applied at times  $t = 0, u_1, u_2, \dots, u_n$ ,

$$\epsilon(t) = \sigma_0 D(t) + \sum_{i=1}^n \sigma_i D(t - u_i) \quad (4-55)$$

If the loaded specimen is allowed to elongate for some time and the stress is then removed, creep recovery will be observed. An uncross-linked amorphous polymer approximates a highly viscous fluid in such a mechanical test. Hence the elongation-time curve of Fig. 1-3c is fitted by an equation of the form

$$\epsilon(t) = \sigma_0 [D(t) - D(t - u_1)] \quad (4-56)$$

Here a stress  $\sigma_0$  is applied at  $t = 0$  and removed at  $t = u_1$ . (This is equivalent to the application of an additional stress equal to  $-\sigma_0$ .)

**EXAMPLE 4-2**

A particular grade of polypropylene has the following tensile creep compliance when measured at 35 °C:  $D(t) = 1.2 t^{0.1} \text{ GPa}^{-1}$ , where  $t$  is in seconds. The polymer is subjected to the following time sequence of tensile stresses at 35 °C.

$$\begin{aligned} \sigma &= 0 & t < 0 \\ \sigma &= 1 \text{ MPa } (10^{-3} \text{ GPa}) & 0 \leq t < 2000 \text{ s} \\ \sigma &= 1.5 \text{ MPa } (1.5 \times 10^{-3} \text{ GPa}) & 1000 \leq t < 2000 \text{ s} \\ \sigma &= 0 & t \geq 2000 \end{aligned}$$

Find the tensile strain at 1500 s and 2500 s using the Boltzmann superposition principle.

At  $t = 1500$  s, the total tensile strain  $\epsilon(1500) = \epsilon_0(1500) + \epsilon_1(1500)$  (Eq. 4-54).

Here,  $\epsilon_0(1500) = 10^{-3} \times 1.2 \times (1500)^{0.1}$  and  $\epsilon_1(1500) = 1.5 \times 10^{-3} \times 1.2 \times (1500 - 1000)^{0.1}$ .

Therefore,  $\epsilon(1500) = 5.84 \times 10^{-3}$ .

At  $t = 2500$  s, the total tensile strain  $\epsilon(2500) = \epsilon_0(2500) + \epsilon_1(2500) - \epsilon_2(2500)$  (Eqs. 4-55 and 4-56).

Here,  $\epsilon_0(2500) = 10^{-3} \times 1.2 \times (2500)^{0.1}$ ,  $\epsilon_1(2500) = 10^{-3} \times 1.2 \times (2500 - 1000)^{0.1}$  and  $\epsilon_2(2500) = (1 + 1.5) \times 10^{-3} \times 1.2 \times (2500 - 2000)^{0.1}$ .

Therefore,  $\epsilon(2500) = 0.78 \times 10^{-3}$ .

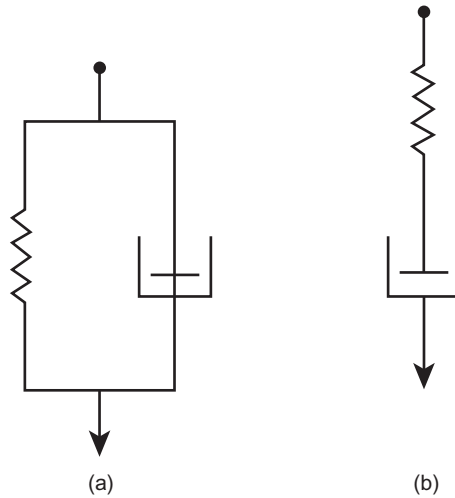
**4.7.2.2 Use of Mechanical Models**

Equation (4-36) summarized purely elastic response in tension. The analogous expression for shear deformation (Fig. 4.14) is

$$\tau = G\gamma \quad (4-57)$$

This equation can be combined conceptually with the viscous behavior of Eq. (4-39) in either of two ways. If the stresses causing elastic extension and viscous flow are considered to be additive, then

$$\tau = \tau_{\text{elastic}} + \tau_{\text{viscous}} = G\gamma + \eta d\gamma/dt \quad (4-58)$$

**FIGURE 4.18**

Simple mechanical models of viscoelastic behavior. (a) Voigt or Kelvin element and (b) Maxwell element.

A mechanical model for such response would include a parallel arrangement of a spring for elastic behavior and a dashpot for the viscous component. (A dashpot is a piston inside a container filled with a viscous liquid.) This model, shown in Fig. 4.18a, is called a Kelvin or a Voigt element. When a force is applied across such a model, the stress is divided between the two components and the elongation of each is equal.

Another way to combine the responses of Eqs. (4-39) and (4-57) is to add the strains. Then

$$\begin{aligned} \gamma &= \gamma_{\text{elastic}} + \gamma_{\text{viscous}} \\ \frac{d\gamma}{dt} &= \frac{d\gamma_{\text{elastic}}}{kt} + \frac{d\gamma_{\text{elastic}}}{dt} = \frac{1}{G} \frac{d\tau}{dt} + \frac{\tau}{\eta} \end{aligned} \quad (4-59)$$

The mechanical analog for this behavior is a spring and dashpot in series. This body, called a Maxwell element, is shown in Fig. 4.18b.

Mechanical models are useful tools for selecting appropriate mathematical functions to describe particular phenomena. The models have no physical relation to real materials, and it should be realized that an infinite number of different models can be used to represent a given phenomenon. Two models are mentioned here to introduce the reader to such concepts, which are widely used in studies of viscoelastic behavior.

The Maxwell body is appropriate for the description of stress relaxation, while the Voigt element is more suitable for creep deformation. It is worth noting that

the Maxwell element can also be solved (Eq. 4-59) for creep deformation. However, the resultant equations do not describe creep deformation well. Therefore, they are seldom used in practice. On the other hand, the Voigt element cannot be solved (Eq. 4-58) in a meaningful way for stress relaxation (an instantaneous strain is applied at  $t = 0$ ) because the dashpot cannot be deformed instantaneously. In a stress relaxation experiment, a strain  $\gamma_0$  is imposed at  $t = 0$  and held constant thereafter ( $d\gamma/dt = 0$ ) while  $\tau$  is monitored as a function of  $t$ . Under these conditions, Eq. (4-59) for a Maxwell body behavior becomes

$$0 = \frac{1}{G} \frac{d\tau}{dt} + \frac{\tau}{\eta} \quad (4-60)$$

This is a first-order homogeneous differential equation and its solution is

$$\tau = \tau_0 \exp(-Gt/\eta) \quad (4-61)$$

where  $\tau_0$  is the initial value of stress at  $\gamma = \gamma_0$ .

Another way of writing Eq. (4-59) is

$$\frac{dy}{dt} = \frac{1}{G} \frac{d\tau}{dt} + \frac{\tau}{\zeta G} \quad (4-62)$$

where  $\zeta$  (zeta) is a relaxation time defined as

$$\zeta \equiv \eta/G \quad (4-63)$$

An alternative form of Eq. (4-61) is then

$$\tau = \tau_0 \exp(-t/\zeta) \quad (4-64)$$

The relaxation time is the time needed for the initial stress to decay to  $1/e$  of its initial value.

If a constant stress  $\tau_0$  were applied to a Maxwell element, the strain would be

$$\gamma = \tau_0/G + \tau_0 t/\eta \quad (4-65)$$

This equation is derived by integrating Eq. (4-59) with boundary condition  $\gamma = 0$ ,  $\tau = \tau_0$  at  $t = 0$ . Although the model has some elastic character the viscous response dominates at all but short times. For this reason, the element is known as a *Maxwell fluid*.

A simple creep experiment involves application of a stress  $\tau_0$  at time  $t = 0$  and measurement of the strain while the stress is held constant. The Voigt model (Eq. 4-58) is then

$$\tau_0 = G\gamma + \eta dy/dt \quad (4-66)$$

or

$$\frac{\tau_0}{\eta} = \frac{G\gamma}{\eta} + \frac{d\gamma}{dt} = \frac{\gamma}{\zeta} + \frac{d\gamma}{dt} \quad (4-67)$$

where  $\zeta = G/\eta$  is called a *retardation time* in a creep experiment. Equation (4-67) can be made exact by using the multiplying factor  $e^{t/\zeta}$ . Integration from  $\tau = \tau_0$ ,  $\gamma = 0$  at  $t = 0$  gives

$$G\gamma/\tau_0 = 1 - \exp(-Gt/\eta) = 1 - \exp(-t/\zeta) \quad (4-68)$$

If the creep experiment is extended to infinite times, the strain in this element does not grow indefinitely but approaches an asymptotic value equal to  $\tau_0/G$ . This is almost the behavior of an ideal elastic solid as described in Eq. (4-36) or (4-57). The difference is that the strain does not assume its final value immediately on imposition of the stress but approaches its limiting value gradually. This mechanical model exhibits delayed elasticity and is sometimes known as a *Kelvin solid*. Similarly, in creep recovery the Maxwell body will retract instantaneously, but not completely, whereas the Voigt model recovery is gradual but complete.

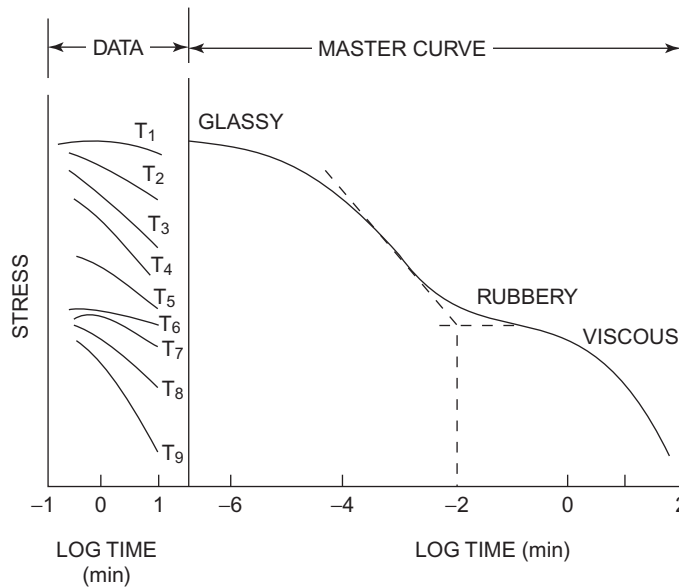
Neither simple mechanical model approximates the behavior of real polymeric materials very well. The Kelvin element does not display stress relaxation under constant strain conditions and the Maxwell model does not exhibit full recovery of strain when the stress is removed. A combination of the two mechanical models can be used, however, to represent both the creep and stress relaxation behaviors of polymers. This is the standard linear solid, or Zener model, comprising either a spring in series with a Kelvin element or a spring in parallel with a Maxwell model. Details of this construction are outside the scope of this introductory text.

Limitations to the effectiveness of mechanical models occur because actual polymers are characterized by many relaxation times instead of single values and because use of the models mentioned assumes linear viscoelastic behavior which is observed only at small levels of stress and strain. The linear elements are nevertheless useful in constructing appropriate mathematical expressions for viscoelastic behavior and for understanding such phenomena.

#### 4.7.2.3 Time–Temperature Correspondence

The left-hand panel of Fig. 4.19 contains sketches of typical stress relaxation curves for an amorphous polymer at a fixed initial strain and a series of temperatures. Such data can be obtained much more conveniently than those in the experiment summarized in Fig. 4.8, where the modulus was measured at a given time and a series of temperatures. It is found that the stress relaxation curves can be caused to coincide by shifting them along the time axis. This is shown in the right-hand panel of Fig. 4.19 where all the curves except that for temperature  $T_8$  have been shifted horizontally to form a continuous “master curve” at temperature  $T_8$ . The glass transition temperature is shown here to be  $T_5$  at a time of  $10^{-2}$  min. The polymer behaves in a glassy manner at this temperature when a strain is imposed within  $10^{-2}$  min or less.

Similar curves can be constructed for creep or dynamic mechanical test data of amorphous polymers. Because of the equivalence of time and temperature, the

**FIGURE 4.19**

Left panel: Stress decay at various temperatures  $T_1 < T_2 < \dots < T_9$ . right panel: Master curve for stress decay at temperature  $T_8$ .

temperature scale in dynamic mechanical experiments can be replaced by an inverse log frequency scale.

Master curves permit the evaluation of mechanical responses at very long times by increasing the test temperature instead of prolonging the experiment. A complete picture of the behavior of the material is obtained in principle by operating in experimentally accessible time scales and varying temperatures.

Time–temperature superposition can be expressed mathematically as

$$G(T_1, t) = G(T_2, t/a_T) \quad (4-69)$$

for a shear stress relaxation experiment. The effect of changing the temperature is the same as multiplying the time scale by shift factor  $a_T$ . A minor correction is required to the formulation of Eq. (4-69) to make the procedure complete. The elastic modulus of a rubber is proportional to the absolute temperature  $T$  and to the density  $\rho$  of the material, as summarized in Eq. (4-31). It is therefore proper to divide through by  $T$  and  $\rho$  to compensate for these effects of changing the test temperature. The final expression is then

$$\frac{G(T_1, t)}{\rho(T_1)T_1} = \frac{G(T_2, t/a_T)}{\rho(T_2)T_2} \quad (4-70)$$

If a compliance were being measured at a series of temperatures  $T$ , the data could be reduced to a reference temperature  $T$  by

$$J(T_1, t) = \frac{\rho(T)T}{\rho(T_1)T_1} J\left(\frac{T, t}{a_T}\right) \quad (4-71)$$

where  $\rho(T_1)$  is the material density at temperature  $T_1$ .

It is common practice now to use the glass transition temperature measured by a very slow rate method as the reference temperature for master curve construction. Then the shift factor for most amorphous polymers is given fairly well by

$$\log_{10} a_T = -\frac{C_1(T - T_g)}{C_2 + T - T_g} \quad (4-72)$$

where the temperatures are in Kelvin. Equation (4-72) is known as the WLF equation, after the initials of the researchers who proposed it [7]. The constants  $C_1$  and  $C_2$  depend on the material. “Universal” values are  $C_1 = 17.4$  and  $C_2 = 51.6$  °C. The expression given holds between  $T_g$  and  $T_g + 100$  °C. If a different reference temperature is chosen, an equation with the same form as Eq. (4-72) can be used, but the constants on the right-hand side must be reevaluated.

Accumulation of long-term data for design with plastics can be very inconvenient and expensive. The equivalence of time and temperature allows information about mechanical behavior at one temperature to be extended to longer times by using data from shorter time studies at higher temperature. It should be used with caution, however, because the increase of temperature may promote changes in the material, such as crystallization or relaxation of fabrication stresses that affect mechanical behavior in an irreversible and unexpected manner. Note also that the master curve in the previous figure is a semilog representation. Data such as that in the left-hand panel is usually readily shifted into a common relation but it is not always easy to recover accurate stress level values from the master curve when the time scale is so compressed.

The following simple calculation illustrates the very significant temperature and time dependence of viscoelastic properties of polymers. It serves as a convenient, but less accurate, substitute for the accumulation of the large amount of data needed for generation of master curves.

### EXAMPLE 4-3

Suppose that a value is needed for the compliance (or modulus) of a plastic article for 10 years' service at 25 °C. What measurement time at 80 °C will produce an equivalent figure? We rely here on the use of a shift factor,  $a_T$ , and Eq. (4-69). Assume that the temperature dependence of the shift factor can be approximated by an Arrhenius expression of the form

$$a_T = \exp \frac{\Delta H}{R} \left[ \frac{1}{T} - \frac{1}{T_0} \right]$$

where the activation energy,  $\Delta H$ , may be taken as 0.12 MJ/mol, which is a typical value for relaxations in semicrystalline polymers and in glassy polymers at temperatures below  $T_g$ . (The shift factor could also have been calculated from the WLF relation if the temperatures had been around  $T_g$  of the polymer.) In the present case:

$$a_T = \exp \left[ \frac{0.12 \times 10^6}{8.31} \right] \left[ \frac{1}{353} - \frac{1}{298} \right] = 0.53 \times 10^{-3}$$

The measurement time required at 80 °C is  $[0.53 \times 10^{-0}]$  [10 years] [365 days/year] [24 hours/day] = 45.3 hours, to approximate 10 years' service at 25 °C.

## 4.8 Dynamic Mechanical Behavior at Thermal Transitions

The storage modulus  $G'(\omega)$  behaves like a modulus measured in a static test and decreases in the glass transition region (cf. Fig. 4.8). The loss modulus  $G''(\omega)$  and  $\tan \delta$  go through a maximum under the same conditions, however. Figure 4.20 shows some typical experimental data.  $T_g$  can be identified as the peak in the  $\tan \delta$  or the loss modulus trace. These maxima do not coincide exactly. The maximum in  $\tan \delta$  is at a higher temperature than that in  $G''(\omega)$ , because  $\tan \delta$  is the ratio of  $G'(\omega)$  and  $G''(\omega)$  (Eq. 4-49) and both these moduli are changing in the transition region. At low frequencies (about 1 Hz) the peak in  $\tan \delta$  is about 5 °C warmer than  $T_g$  from static measurements or the maximum in the loss modulus–temperature curve.

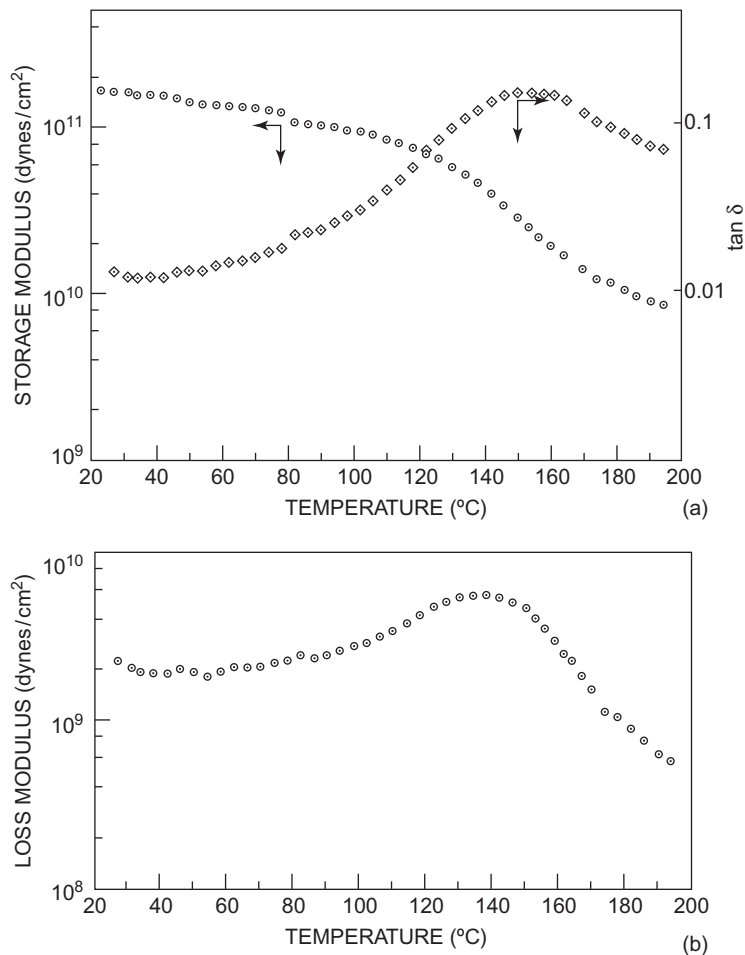
The development of a maximum in  $\tan \delta$  or the loss modulus at the glass-to-rubber transition is explained as follows. At temperatures below  $T_g$  the polymer behaves elastically, and there is little or no flow to convert the applied energy into internal work in the material. Now  $h$ , the energy dissipated as heat per unit volume of material per unit time because of flow in shear deformation, is

$$h = \tau d\gamma/dt = \eta(d\gamma/dt)^2 \quad (4-73)$$

[To check this equation by dimensional analysis in terms of the fundamental units mass ( $m$ ), length ( $l$ ), and time ( $t$ ):

$$\begin{aligned} \tau &= ml^{-1}t^{-2}, & d\gamma/dt &= t^{-1}, & \eta &= ml^{-1}t^{-1}, & \text{force} &= mlt^{-2}, \\ \text{work} &= ml^2t^{-2}, & \text{work/volume/time} &= ml^{-1}t^{-3} = \text{Eq. (4-73)}. \end{aligned}$$

Thus the work dissipated is proportional to the viscosity of the material at fixed straining rate  $d\gamma/dt$ . At low temperatures,  $\eta$  is very high but  $\gamma$  and  $d\gamma/dt$  are vanishingly small and  $h$  is negligible. As the structure is loosened in the transition region,  $\eta$  decreases but  $d\gamma/dt$  becomes much more significant so that  $h$  (and the loss modulus and  $\tan \delta$ ) increases. The effective straining rate of polymer segments continues to increase somewhat with temperature above  $T_g$  but  $\eta$ , which measures the resistance to flow, decreases at the same time. The net result is a diminution of damping and a fall-off of the magnitudes of the storage modulus and  $\tan \delta$ .

**FIGURE 4.20**

(a) Storage modulus and  $\tan \delta$  of an oriented poly(ethylene terephthalate) fiber. 11-Hz frequency. (b) Loss modulus of the same fiber.

**EXAMPLE 4-4**

An interesting application of dynamic mechanical data is in blends of rubbers for tire treads. Rolling is at low frequencies, while skidding is at high frequencies. (Compare the hum of tires on the pavement with the screech of a skid.) Therefore, low rolling friction requires low damping (i.e., little dissipation of mechanical energy) at low frequencies while skid resistance implies high damping at higher frequencies. One way to achieve the desired property balance is to blend elastomers with the respective properties.

### 4.8.1 Relaxations at Temperatures below $T_g$

In the glass transition region, the storage modulus of an amorphous polymer drops by a factor of  $\sim 1000$ , and  $\tan \delta$  is generally one or more. (The  $\tan \delta$  in Fig. 4.20a is less than this because the polymer is oriented and partially crystalline.) In addition to  $T_g$ , minor transitions are often observed at lower temperatures, where the modulus may decrease by a factor of  $\sim 2$  and  $\tan \delta$  has maxima of 0.1 or less. These so-called **secondary transitions** arise from the motions of side groups or segments of the main chain that are smaller than those involved in the displacements associated with  $T_g$ . Secondary transitions increase in temperature with increasing frequency in a manner similar to the main glass transition. They can be detected by dynamic mechanical and also by dielectric loss factor and nuclear magnetic resonance measurements.

Some amorphous polymers are not brittle at temperatures below  $T_g$ . Nearly all these tough glasses have pronounced secondary transitions. Figure 4.21 is a sketch of the temperature dependence of the shear storage and loss moduli for polycarbonate [8], which is one such polymer. The molecular motions that are responsible for the ductile behavior of some glassy polymers are probably associated with limited range motions of main chain segments. Polymers like poly(methyl methacrylate) that exhibit secondary transitions due to side group motions are not particularly tough.

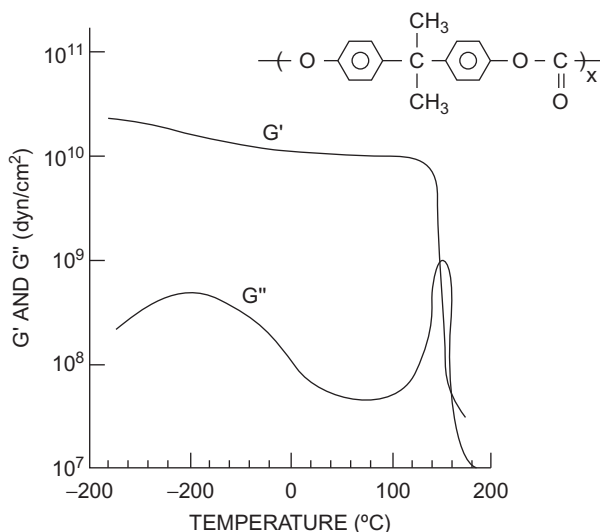


**FIGURE 4.21**

Storage ( $G'$ ) and loss ( $G''$ ) moduli of polycarbonate polymer [8]. The broad low-temperature peak is probably composed of several overlapping maxima.

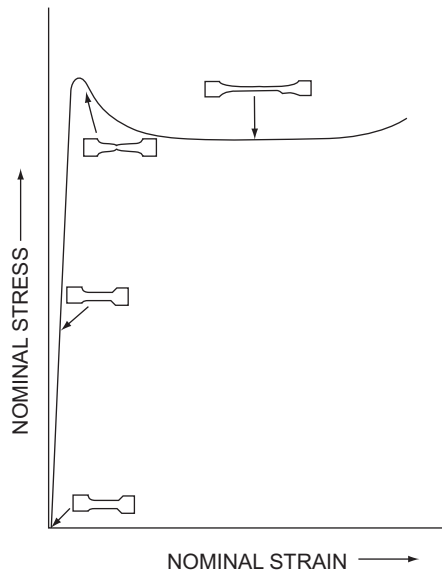
## 4.9 Stress–Strain Tests

Stress-strain tests were mentioned in Section 1.8 and in Fig. 4.14. In such a tensile test a parallel-sided strip is held in two clamps that are separated at a constant speed, and the force needed to effect this is recorded as a function of clamp separation. The test specimens are usually dogbone shaped to promote deformation between the clamps and deter flow in the clamped portions of the material. The load-elongation data are converted to a stress–strain curve using the relations mentioned in Section 1.8. These are probably the most widely used of all mechanical tests on polymers. They provide useful information on the behavior of isotropic specimens, but their relation to the use of articles fabricated from the same polymer as the test specimens is generally not straightforward. This is because such articles are anisotropic, their properties may depend strongly on the fabrication history, and the use conditions may vary from those in the tensile test. Stress–strain tests are discussed here, with the above cautions, because workers in the field often develop an intuitive feeling for the value of such data with particular polymers and because they provide useful general examples of the effects of testing rate and temperature in mechanical testing.

Dynamic mechanical measurements are performed at very small strains in order to ensure that linear viscoelasticity relations can be applied to the data. Stress–strain data involve large strain behavior and are accumulated in the non-linear region. In other words, the tensile test itself alters the structure of the test specimen, which usually cannot be cycled back to its initial state. (Similarly, dynamic deformations at large strains test the fatigue resistance of the material.)

Figure 1.2 records some typical stress–strain curves for different polymer types. Some polymers exhibit a yield maximum in the nominal stress, as shown in part (c) of the figure. At stresses lower than the yield value, the sample deforms homogeneously. It begins to neck down at the yield stress, however, as sketched in Fig. 4.22. The necked region in some polymers stabilizes at a particular reduced diameter, and deformation continues at a more or less constant nominal stress until the neck has propagated across the whole gauge length. The cross-section of the necking portion of the specimen decreases with increasing extension, so the true stress may be increasing while the total force and the nominal stress (Section 1.8) are constant or even decreasing. The process described is variously called yielding, necking, cold flow, and cold-drawing. It is involved in the orientation processes used to confer high strengths on thermoplastic fibers. Tough plastics always exhibit significant amounts of yielding when they are deformed. This process absorbs impact energy without causing fracture of the article. Brittle plastics have a stress–strain curve like that in Fig. 1.2b and do not cold flow to any noticeable extent under impact conditions. Many partially crystalline plastics yield in tensile tests at room temperature but this behavior is not confined to such materials.

The yield stress of amorphous polymers is found to decrease linearly with temperature until it becomes almost zero near  $T_g$ . Similarly, the yield stress of

**FIGURE 4.22**

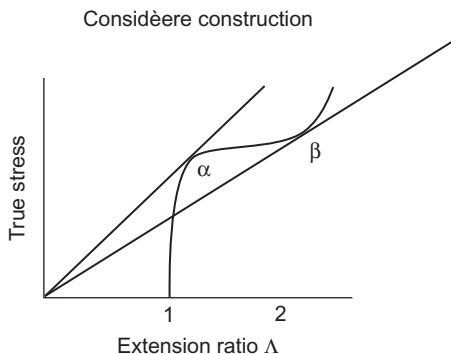
Tensile stress–strain curve and test specimen appearance for a polymer which yields and cold draws.

partially crystalline materials becomes vanishingly small near  $T_m$ , as the crystallites that hold the macromolecules in position are melted out. Yield stresses are rate dependent and increase at faster deformation rates.

The shear component of the applied stress appears to be the major factor in causing yielding. The uniaxial tensile stress in a conventional stress–strain experiment can be resolved into a shear stress and a dilational (negative compressive) stress normal to the parallel sides of test specimens of the type shown in Fig. 4.22. Yielding occurs when the shear strain energy reaches a critical value that depends on the material, according to the von Mises yield criterion, which applies fairly well to polymers.

Yield and necking phenomena can be envisioned usefully with the Considère construction shown in Fig. 4.23. Here the initial conditions are initial gauge length and cross-sectional area  $l_i$  and  $A_i$ , respectively, and the conditions at any instant in the tensile deformation are length  $l$  and cross-sectional area  $A$ , when the force applied is  $F$ . The true stress,  $\sigma_r$ , defined as the force divided by the corresponding instantaneous cross-sectional area  $A_i$ , is plotted against the extension ratio,  $\Lambda$  ( $\Lambda = 1/10 = \epsilon - 1$ , as defined in Fig. 4.14). If the deformation takes place at constant volume then:

$$A_i l_i = A l \quad (4-74)$$

**FIGURE 4.23**

Sketch of conditions for yielding in tensile deformation.

The nominal stress (engineering stress)  $= \sigma = F/A_i$ , and therefore:

$$\sigma = \sigma_t / \Lambda \quad (4-75)$$

$$\frac{d\sigma}{d\Lambda} = \frac{1}{\Lambda} \frac{d\sigma_t}{d\Lambda} - \frac{\sigma_t}{\Lambda^2} \quad (4-76)$$

Since  $d\epsilon = d\Lambda$ , then at yield

$$\frac{d\sigma}{d\epsilon} = 0 = \frac{d\sigma}{d\Lambda} \quad (4-77)$$

and the yield condition is characterized by:

$$\frac{d\sigma_t}{d\Lambda} = \frac{\sigma_t}{\Lambda} \quad (4-78)$$

A maximum in the plot of *engineering* stress against strain occurs only if a tangent can be drawn from  $\lambda = 0$  to touch the curve of *true* stress against the extension ratio at a point, labeled  $\alpha$  in Fig. 4.23. In this figure a second tangent through the origin touches the curve at point  $\beta$ . This defines a minimum in the usual plot of nominal stress against extension ratio where the orientation induced by the deformation stiffens the polymer in the necked region. This phenomenon is called *strain hardening*. The neck stabilizes and travels through the specimen by incorporating more material from the neighboring tapered regions. As the tensile deformation proceeds, the whole parallel gauge length of the specimen will yield. If the true stress-extension ratio relation is such that a second tangent cannot be drawn, the material will continue to thin until it breaks. Molten glass exhibits this behavior.

The phenomenon of strain hardening in polymers is a consequence of orientation of molecular chains in the stretch direction. If the necked material is a

semicrystalline polymer, like polyethylene or a crystallizable polyester or nylon, the crystallite structure will change during yielding. Initial spherulitic or row nucleated structures will be disrupted by sliding of crystallites and lamellae, to yield morphologies like that shown in Fig. 4.7.

Yielding and strain hardening are characteristic of some metals as well as polymers. Polymer behavior differs, however, in two features. One is the temperature rise that can occur in the necked region as a result of the viscous dissipation of mechanical energy and orientation-induced crystallization. The other feature is an increase of the yield stress at higher strain rates. These opposing effects can be quite significant, especially at the high strain rates characteristic of industrial orientation processes for fibers and films.

#### 4.9.1 Rate and Temperature Effects

Most polymers tend to become more rigid and brittle with increasing straining rates. In tensile tests, the modulus (initial slope of the stress–strain curve) and yield stress rise and the elongation at fracture drops as the rate of elongation is increased. Figure 4.24 shows typical curves for a polymer that yields at low straining rates. The work to rupture, which is the area under the stress–strain curve, is a measure of the toughness of the specimen under the testing conditions. This parameter decreases at faster extension rates.

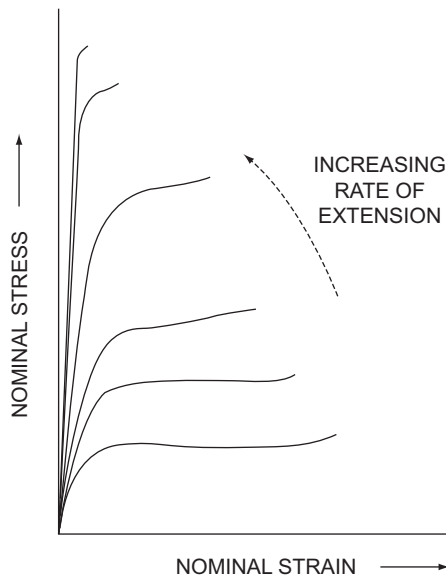


**FIGURE 4.24**

Effect of strain rate on the tensile stress–strain curve of a polymer which yields at low straining rates.

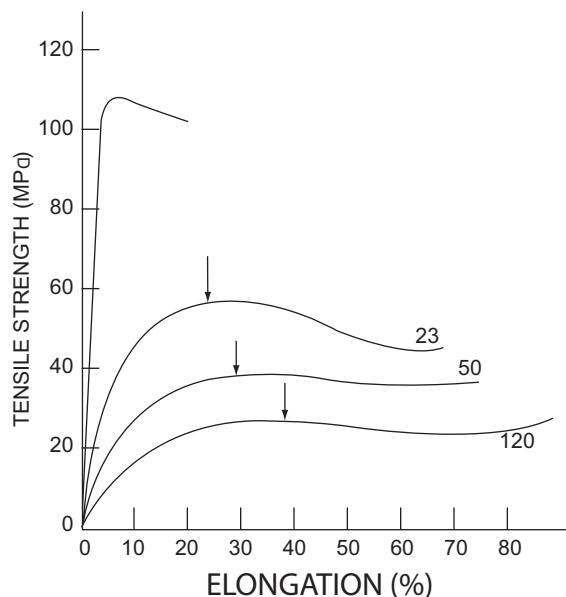


**FIGURE 4.25**

Tensile stress–strain behavior for a molded sample of a nylon-6,6 at the indicated temperatures ( $^{\circ}\text{C}$ ). The arrows indicate the yield points which become more diffuse at higher temperatures.

The influence of temperature on the stress–strain behavior of polymers is generally opposite to that of straining rates. This is not surprising in view of the correspondence of time and temperature in the linear viscoelastic region (Section 4.7.2.3). The curves in Fig. 4.25 are representative of the behavior of a partially crystalline plastic.

#### 4.10 Crazing in Glassy Polymers

When a polymer sample is deformed, some of the applied energy can be dissipated by movement of sections of polymer molecules past each other. This yielding process uses energy that might otherwise be available to enlarge preexisting micro cracks into new fracture surfaces. The two major mechanisms for energy dissipation in glassy polymers are crazing and shear yielding.

Crazes are pseudocracks that form at right angles to the applied load and that are traversed by many microfibrils of polymer that has been oriented in the stress direction. This orientation itself is due to shear flow. Energy is absorbed during the crazing process by the creation of new surfaces and by

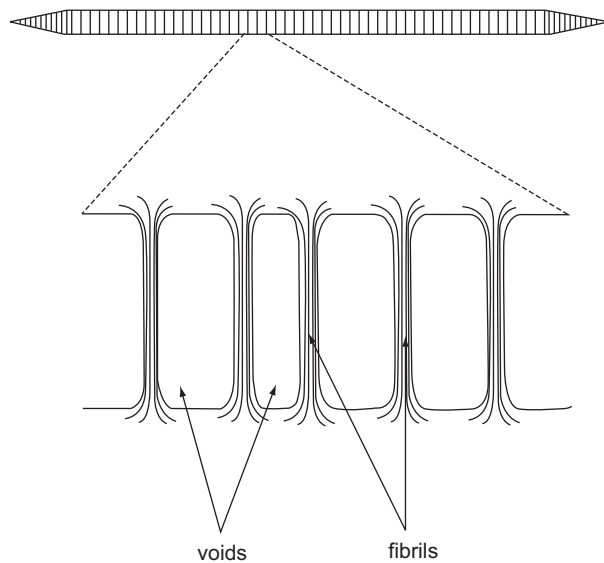


**FIGURE 4.26**

Sketch of a craze in polystyrene [9]. The upper figure shows a craze, with connecting fibrils between the two surfaces. The lower figure is a magnification of a section of the craze showing voids and fibrils. Actual crazes in this polymer are about  $0.1\text{--}2\ \mu\text{m}$  thick; this figure is not to scale.

viscous flow of polymer segments. Although crazes appear to be a fine network of cracks, the surfaces of each craze are connected by oriented polymeric structures and a completely crazed specimen can continue to sustain appreciable stresses without failure. Crazing detracts from clarity, as in poly(methyl methacrylate) signage or windows, and enhances permeability in products such as plastic pipe. Mainly, however, it functions as an energy sink to inhibit or retard fracture.

The term *crazing* is apparently derived from an Anglo-Saxon verb *krasen*, meaning “to break.” In this process polymer segments are drawn out of the adjoining bulk material to form cavitated regions in which the uncrazed surfaces are joined by oriented polymer fibrils, as depicted in Fig. 4.26. Material cohesiveness in amorphous glassy polymers, like polystyrene, arises mainly through entanglements between macromolecules and entanglements are indeed essential for craze formation and craze fibril strength in such polymers [9].

Glassy polymers with higher cohesiveness, like polycarbonate and cross-linked epoxies, preferentially exhibit shear yielding [10], and some materials, such as rubber-modified polypropylene, can either craze or shear yield, depending on the deformation conditions [11]. Application of a stress imparts energy to a

body which can be dissipated either by complete recovery (on removal of the load), by catastrophic rupture, or by polymer flow in the stress application region. The latter process, called shear yielding, or shear banding, is a useful mechanism for absorbing impact forces.

A few comments on the distinction between crazing and shear yielding may be appropriate here. A material which undergoes shear yielding is essentially elastic at stresses up to the yield point. Then it suffers a permanent deformation. There is effectively no change in the volume of the material in this process. In crazing, the first craze initiates at a local stress less than the shear stress of the bulk material. The stress required to initiate a craze depends primarily on the presence of stress-raising imperfections, such as crack tips or inclusions, in the stressed substance, whereas the yield stress in shear is not sensitive to such influences. Permanent deformation in crazing results from fibrillation of the polymer in the stress direction.

Craze formation is a dominant mechanism in the toughening of glassy polymers by elastomers in “polyblends.” Examples are high-impact polystyrene (HIPS), impact poly(vinyl chloride), and ABS (acrylonitrile-butadiene-styrene) polymers. Polystyrene and styrene-acrylonitrile (SAN) copolymers fracture at strains of  $\sim 10^{-2}$ , whereas rubber-modified grades of these polymers (e.g., HIPS and ABS) form many crazes before breaking at strains around 0.5. Rubbery particles in polyblends act as stress concentrators to produce many craze cracks and to induce orientation of the adjacent rigid polymer matrix. Good adhesion between the glassy polymer and rubbery inclusion is important so that cracks do not form and run between the rubber particles. Crazes and yielding are usually initiated at the equators of rubber particles, which are the loci of maximum stress concentration in stressed specimens, because of their modulus difference from the matrix polymer. Crazes grow outward from rubber particles until they terminate on reaching other particles. The rubber particles and crazes will be able to hold the matrix polymer together, preventing formation of a crack, as long as the applied stress is not catastrophic. The main factors that promote craze formation are a high rubber particle phase volume, good rubber-matrix polymer adhesion, and an appropriate rubber particle diameter [12,13]. The latter factor varies with the matrix polymer, being about  $2\ \mu\text{m}$  for polystyrene and about one-tenth of that value for unplasticized PVC. It is intuitively obvious that good adhesion between rubber and matrix polymer is required for transmission of stresses across phase boundaries. Another interesting result stems from the differences in thermal expansion coefficients of the rubber and glassy matrix polymer. For the latter polymers the coefficient of linear expansion (as defined by ASTM method D696) is  $\sim 10^{-6}\ \text{K}^{-1}$ , while the corresponding value for elastomers is  $\sim 10^{-2}\ \text{K}^{-1}$ . When molded samples of rubber-modified polymers are cooled from the melt state the elastomer phase will undergo volume dilation. This increases the openness of the rubber structure and causes a shift of the  $T_g$  of the rubber to lower values than that of unattached elastomer [14].

## 4.11 Fracture Mechanics

This discipline is based on the premise that all materials contain flaws and that fracture occurs by stress-induced extension of these defects. The theory derives from the work of A. E. Griffith [15], who attempted to explain the observation that the tensile strengths (defined as breaking force  $\div$  initial cross-sectional area) of fine glass filaments were inversely proportional to the sample diameter. He assumed that every object contained flaws, that failure is more likely the larger the defect, and that larger bodies would break at lower tensile stresses because they contained larger cracks. The basic concept is that a crack will grow only if the total energy of the body is lowered thereby. That is to say, the elastic strain energy which is relieved by crack growth must exceed the energy of the newly created surfaces. It is important to note also that the presence of a crack or inclusion changes the stress distribution around it, and the stress may be amplified greatly around the tips of sharp cracks. The relation that was derived between crack size and failure stress is known as the Griffith criterion:

$$\sigma_f = \left[ \frac{2\gamma Y}{\pi a} \right]^{1/2} \quad (4-79)$$

where  $\sigma_f$  = failure stress, based on the initial cross-section,  $a$  = crack depth,  $Y$  = tensile (Young's) modulus, and  $\gamma$  = surface energy of the solid material (the factor 2 is inserted because fracture generates two new surfaces). This equation applies to completely elastic fractures; all the applied energy is consumed in generating the fracture surfaces. Real materials are very seldom completely elastic, however, and a more general application of this concept allows for additional energy dissipation in a small plastic deformation region near the crack tip. With this amendment, Eq. (4-79) is applicable with the  $2\gamma$  term replaced by  $G$ , the *strain energy release rate*, which includes both plastic and elastic surface work done in extending a preexisting crack [15]:

$$\sigma_f = \left[ \frac{YG}{\pi a} \right]^{1/2} \quad (4-80)$$

The general equation to describe the applied stress field around a crack tip is [16]:

$$\sigma = \frac{K}{[\pi a]^{1/2}} \quad (4-81)$$

where  $K$  is the stress intensity factor and  $\sigma$  is the local stress. Equation (4-81) applies at all stresses, but the stress intensity reaches a critical value,  $K_c$ , at the stress level where the crack begins to grow.  $K_c$  is a material property, called the *fracture toughness*, and the corresponding strain energy release rate becomes the *critical strain energy release rate*,  $G_c$ .

The equations cited above are for an ideal semi-infinite plate, with no boundary effects. Application to real specimens requires calibration factors, so that the fracture toughness of Eq. (4-81), at the critical point is given by:

$$K_c = \sigma_f \Gamma [\pi a]^{1/2} \quad (4-82)$$

where  $\Gamma$  (gamma) is a calibration factor which is itself a function of specimen geometry and crack size. The  $\Gamma$  values have been tabulated (mainly for metals) for a variety of shapes [17]. The independent variable in Eq. (4-82) is the crack depth,  $a$ . To measure  $K_c$ , sharp cracks of various known depths are made in specimens with fixed geometry and plots of  $\sqrt{a}$  versus  $\sigma_f \Gamma$  are linear with slope  $K_c$ . Instrumented impact tests yield values for the specimen fracture energy,  $U_f$ . With such data, the critical strain energy release rate can be calculated according to [18]:

$$G_c = \frac{U_f}{BD\phi} \quad (4-83)$$

where  $B$  and  $D$  are the specimen depth and width, respectively, and the calibration factor  $\phi$  is a function of the specimen geometry and the ratio of the crack depth and specimen width. Here again, the independent variable is the crack depth,  $a$ , as manifested in parameter  $\phi$ .

The total work of crack formation equals  $G_c \times$  the crack area. Catastrophic failure is predicted to occur when  $\sigma[\pi a]^{1/2} = [YG_c]^{1/2}$ , or when  $K_c = [YG_c]^{1/2}$ .  $K_c$  and  $G_c$  are the parameters used in *linear elastic fracture mechanics* (LEFM). Both factors are implicitly defined to this point for plane stress conditions. To understand the term *plane stress*, imagine that the applied stress is resolved into three components along Cartesian coordinates; plane stress occurs when one component is equal to 0 (the stress in the direction normal to the plane of the specimen). Such conditions are most likely to occur when the specimen is thin.

This reference to specimen thickness leads to a consideration of the question of why a polymer that is able to yield will be less brittle in thin than in thicker sections. Polycarbonate is an example of such behavior. Recall that yielding occurs at constant volume (tensile specimens neck down on extension). In thin objects the surfaces are load-free and can be drawn inward as a yield zone grows ahead of a crack tip. In a thick specimen the material surrounding the yield zone is at a lower stress than that in the crack region. It is not free to be drawn into the yield zone and acts as a restraint on plastic flow of the region near the crack tip. As a consequence, fracture occurs with a lower level of energy absorption in a thick specimen. The crack tip in a thin specimen will be in a state of plane stress while the corresponding condition in a thick specimen will be plane strain. Plane strain is the more dangerous condition.

The parameters that apply to plane strain fracture are  $G_{Ic}$  and  $K_{Ic}$ , where the subscript I indicates that the crack opening is due to tensile forces.  $K_{Ic}$  is

measured by applying Eq. (4-82) to data obtained with thick specimens. To illustrate the differences between plane stress and plane strain fracture modes, thin polycarbonate specimens with thicknesses  $\leq 3$  mm are reported to have  $G_c$  values of  $10 \text{ kJ/m}^2$ , while the  $G_{Ic}$  of thick specimens is  $1.5 \text{ kJ/m}^2$ . It will be useful to consider a practical application of LEFM here.

#### EXAMPLE 4-5

Consider a study of the effect of preexisting flaws on the ability of PVC pipe to hold pressure [19]. The critical stress intensity factor,  $K_{Ic}$ , is reported to be  $1.08 \text{ MPa} \cdot \text{m}^{1/2}$  for PVC under static load at  $20^\circ\text{C}$ . The stress ( $\sigma$ ) in a pipe = the internal pressure,  $P$ , + the hoop stress at the inner surface:

$$\sigma = P + \frac{P[D - t]}{2t} \quad (4-84)$$

where  $D$  is the outside diameter and  $t$  is the pipe wall thickness. In this case,  $D = 250$  mm and  $t = 17$  mm. For pipe of this type  $\Gamma$  (in Eq. 4-82) is about 1.12 [20]. Assuming that the presence of 1 mm flaws will give a conservative estimate of pipe service life, we take  $a = 1$  mm in Eq. (4-82). The critical stress for failure is

$$\sigma_f = \frac{K_{Ic}}{I[\pi a]^{1/2}} = \frac{1.08 \text{ MPa m}^{1/2}}{1.12[10^{-3}\pi\text{m}]^{1/2}} = 17.2 \text{ MPa}$$

$$\sigma_f = P + \frac{P[D - t]}{2t} = 7.85 P_c$$

where  $P_c$  is the critical pressure for brittle fracture of the pipe. Hence,

$$P_c = \frac{17.2 \text{ MPa}}{7.85} = 2.19 \text{ MPa} = 318 \text{ psi}$$

An otherwise well-made pipe will sustain steady pressures up to 2.19 MPa (318 psi) without failing by brittle fracture if it contains initial flaws as large as 1 mm. Similar calculations show that initial flaws or inclusions smaller than 4.5 mm permit steady operation at 150 psi (1.03 MPa).

LEFM discussed to this point refers to the resistance of bodies to crack growth under static loads. Crack growth under cyclic loading is faster than under static loads at the same stress amplitudes, because the rate of loading and the damage both increase with higher frequencies.

Polymers which yield extensively under stress exhibit nonlinear stress–strain behavior. This invalidates the application of linear elastic fracture mechanics. It is usually assumed that the LEFM approach can be used if the size of the plastic zone is small compared to the dimensions of the object. Alternative concepts have been proposed for rating the fracture resistance of tougher polymers, like polyolefins, but empirical pendulum impact or dart drop tests are deeply entrenched for judging such behavior.

### 4.12 Toughness and Brittleness

Many polymers that yield and exhibit tough, ductile behavior under the conditions of normal tensile tests prove to be brittle when impacted. This is particularly true when the sample contains notches or other stress concentrators. Fracture behavior is characterized by a variety of empirical tests. None of these can be expected to correlate very closely with service performance, because it is very difficult to analyze stress and deformation behavior of complex real articles under the variety of loads that may be encountered in practice. Impact tests aim to rate the fracture resistance of materials by measuring the energy required to break specimens with standard dimensions. The values obtained relate to the experimental conditions and the geometry and history of the specimen. A single figure for impact strength is of limited value in itself but such data can be useful for predicting serviceability of materials for different applications if they are obtained, say, from a series of impact tests at various temperatures and sample shapes and are combined with experience of the performance of similar materials and part shapes under related service conditions.

Impact tests are often used to locate the brittle-ductile temperature or brittleness temperature. This parameter is generally defined as the temperature at which half the specimens tested fail in a given test. Because of the nature of most of these impact tests, this approximates the temperature range in which yielding processes begin to absorb substantial portions of the applied energy. As the test temperature is increased through the brittle-to-tough transition region, the measured impact energies increase substantially and the specimens exhibit more evidence of having flowed before fracturing.

Ductile–brittle transitions are more accurately located by variable temperature tests than by altering impact speed in an experiment at a fixed temperature. This is because a linear fall in temperature is equivalent to a logarithmic increase in straining rate. The ductile–brittle transition concept can be clarified by sketches such as that in Fig. 4.27 [21]. In the brittle region, the impact resistance of a material is related to its LFM properties, as described above. In the mixed mode failure region, fracture resistance is proportional to the size of the yield zone that develops at a crack tip during impact. If the yield zone (also sometimes called a plastic zone) is small, fracture tends to be brittle and can be described by LFM concepts. If yielding takes place on a large scale, then the material will absorb considerable energy before fracturing and its behavior will be described as tough.

The relative importance of the yield zone can be estimated, for a given product, by comparing its yield stress and fracture toughness. The parameter proposed for this purpose is  $[K_{Ic}/\sigma_y]^2$ , where  $\sigma_y$  is the yield stress [22]. This ratio has units of length and has been suggested to be proportional to the size of the yield zone. Higher values indicate tougher materials. In the third region of Fig. 4.27, impact resistance is determined by the capacity of the product to absorb energy by localized necking and related mechanisms, after yielding.

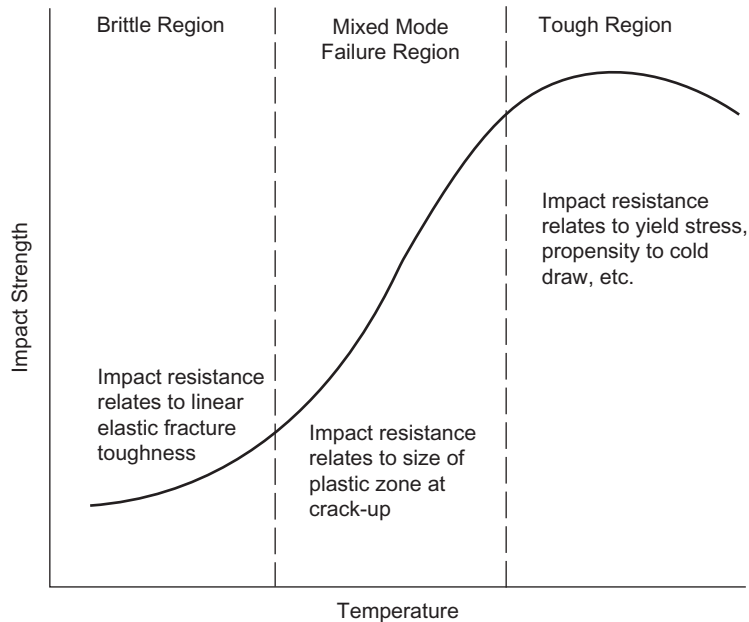


**FIGURE 4.27**

Ductile–brittle behavior in impact resistance [21]. The transition between the zones varies with the rate of impact and type of test.

Notches act as stress raisers and redistribute the applied stress so as to favor brittle fracture over plastic flow. Some polymers are much more notch sensitive than others, but the brittleness temperature depends in general on the test specimen width and notch radius. Polymers with low Poisson ratios tend to be notch sensitive. Comparisons of impact strengths of unnotched and notched specimens are often used as indicators of the relative danger of service failures with complicated articles made from notch sensitive materials.

Weld lines (also known as knit lines) are a potential source of weakness in molded and extruded plastic products. These occur when separate polymer melt flows meet and weld more or less into each other. Knit lines arise from flows around barriers, as in double or multigating and use of inserts in injection molding. The primary source of weld lines in extrusion is flow around spiders (multi-armed devices that hold the extrusion die). The melt temperature and melt elasticity (which is mentioned in the next section of this chapter) have major influences on the mechanical properties of weld lines. The tensile and impact strength of plastics that fail without appreciable yielding may be reduced considerably by double-gated moldings, compared to that of samples without weld lines. Polystyrene and SAN copolymers are typical of such materials. The effects of

weld lines are relatively minor with ductile amorphous plastics like ABS and polycarbonate and with semicrystalline polymers such as polyoxymethylene. This is because these materials can reduce stress concentrations by yielding [23].

Semicrystalline polymers are impact resistant if their glass transition temperatures are much lower than the test temperature. The impact strength of such materials decreases with increasing degree of crystallinity and particularly with increased size of supercrystalline structures like spherulites. This is because these changes are tantamount to the progressive decrease in the numbers of tie molecules between such structures.

The impact strength of highly cross-linked thermoset polymers is little affected by temperature since their behavior is generally glassy in any case.

---

### 4.13 Rheology

Rheology is the study of the deformation and flow of matter. The processing of polymers involves rheological phenomena. They cannot be evaded. It is important, therefore, that practitioners have at least some basic knowledge of this esoteric subject. This section is a very brief review, with the aim of guiding the perplexed to at least ask the right questions when confronted with a rheological problem. Following is a summary of the major points, which are elaborated below.

1. The rheological behavior of materials is generally very complex, and polymers are usually more complex than alternative materials of construction.
2. A complete rheological characterization of a material is very time consuming and expensive and much of the data will be irrelevant to any particular process or problem.
3. Rheological measurements must be tailored to the particular process and problem of interest. This is the key to successful solution of rheological and processing problems. Relevant rheological experiments are best made at the same temperatures, flow rates, and deformation modes that prevail in the process of interest.
4. Following are some important questions that should be asked in the initial stages of enquiry:
  - a. Is the process isothermal? Most standard rheological measurements are isothermal; many processes are not.
  - b. Is the material behavior entirely viscous or does it also comprise elastic components?
  - c. Does processing itself change the rheological properties of the material?
  - d. Do the material purchase specifications ensure rheological behavior?
  - e. Do steady-state rheological measurements characterize the material in a particular process?
  - f. Is it best to look to rheological measurements or to process simulations for answers to a particular problem?

The coefficient of viscosity concept,  $\eta$ , was introduced in connection with Eq. (3-59) as the quotient of the shearing force per unit area divided by the velocity gradient. The numerator here is the shearing stress,  $\tau$ , and the denominator is termed the shear rate,  $\dot{\gamma}$  ( $\gamma$  is the strain and  $\dot{\gamma} \equiv d\gamma/dt$ ). With these changes, Eq. (3-59) reads:

$$\eta = \frac{(F/A)}{(dv/dr)} = \tau\dot{\gamma} \quad (4-85)$$

The viscosity of water at room temperature is  $10^{-3}$  Pa · sec [= 1 centipoise (cP)], while that of molten thermoplastics at their processing temperatures is in the neighborhood of 103–104 Pa · sec. Lubricating oils are characterized by  $\eta$  values up to about 1 Pa · sec. In SI units, the dimensions of viscosity are  $\text{N} \cdot \text{sec}/\text{m}^2 = \text{Pa} \cdot \text{sec}$ .

If  $\eta$  is independent of shear history, the material is said to be time independent. Such liquids can exhibit different behavior patterns, however, if, as is frequently the case with polymers,  $\eta$  varies with shear rate. A material whose viscosity is independent of shear rate, e.g., water, is a Newtonian fluid. Figure 4.28 illustrates shear-thickening, Newtonian, and shear-thinning  $\eta - \dot{\gamma}$  relations. Most polymer melts and solutions are shear-thinning. (Low-molecular-weight polymers and dilute solutions often exhibit Newtonian characteristics.) Wet sand is a familiar example of a shear-thickening substance. It feels hard if you run on it, but you can sink down while standing still.

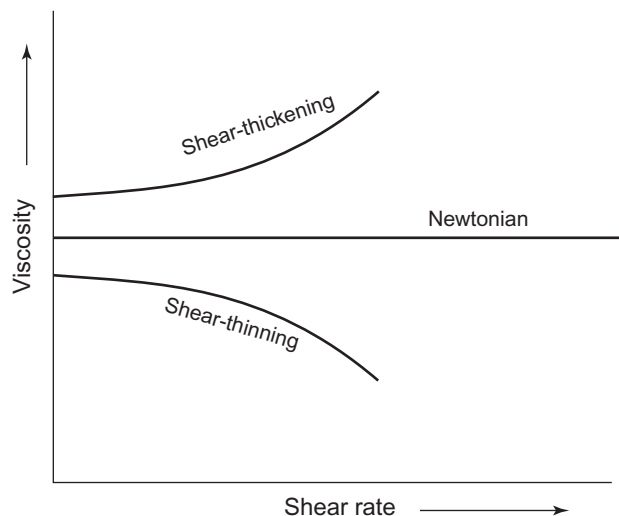


**FIGURE 4.28**

Time-independent fluids.

A single figure for  $\eta$  is not appropriate for non-Newtonian substances, and it is common practice to plot “flow curves” of such materials in terms of  $\eta_a$  (apparent viscosity) against corresponding values of  $\dot{\gamma}$ . Many equations have been proposed to describe non-Newtonian behavior. Generally, however, the mathematics involved is not worth the effort except for the simplest problems. It is most efficient to read the required viscosity values from experimental  $\eta_a - \dot{\gamma}$  plots. These relations can usually be described over limited shear rate ranges by power law expressions of the form:

$$\tau = C(\dot{\gamma})^n \quad (4-86)$$

where  $n$  is the power law index. If  $n < 1$  the material is shear-thinning; if  $n > 1$ , it is shear-thickening. The constant  $C$  has no real physical significance because its units will vary with  $n$ . Equation (4-86) indicates that a log–log plot of  $\tau$  vs.  $\dot{\gamma}$  is linear over the shear rate range of applicability. An alternative expression is

$$\eta_a = \mu(\dot{\gamma})^{n-1} \quad (4-87)$$

where  $\mu$ , sometimes called the consistency, has limited significance since its units also are dependent on  $n$ . This problem can be circumvented by referencing the apparent viscosity to that at a specified shear rate,  $\dot{\gamma}_{\text{aref}}$ , which is conveniently taken as  $1 \text{ sec}^{-1}$ . Then

$$\eta_a = \eta_{\text{aref}} |\dot{\gamma}_a / \dot{\gamma}_{\text{aref}}|^{n-1} \quad (4-88)$$

Substances that do not flow at shear stresses less than a certain level exhibit yield properties. Then

$$\dot{\gamma} = \frac{\tau - \tau_y}{\eta} \quad (4-89)$$

where  $\tau_y$  is the yield stress. The yield stress may be of no significance, as in high-speed extrusion of plastics, or it could be an important property of materials, as in the application of architectural paints and in rotational molding.

Most polymeric substances are time dependent to some extent and  $\eta = \eta(\dot{\gamma}, t)$ , where  $t$  here refers to the time under shear. If shearing causes a decrease in viscosity the material is said to be *thixotropic*; the opposite behavior characterizes a *rheopectic* substance. These patterns are sketched in Fig. 4.29. After shearing has been stopped, time-dependent fluids recover their original condition in due course. PVC plastisols [mixtures of poly(vinyl chloride) emulsion polymers and plasticizers] and some mineral suspensions often exhibit rheopecty. Thixotropy is a necessary feature of house paints, which must be reasonably fluid when they are applied by brushing or rolling, but have to be viscous in the can and shortly after application, in order to minimize pigment settling and sagging, respectively.

A variety of laboratory instruments have been used to measure the viscosity of polymer melts and solutions. The most common types are the coaxial cylinder, cone-and-plate, and capillary viscometers. Figure 4.30 shows a typical flow curve for a thermoplastic melt of a moderate-molecular-weight polymer, along with

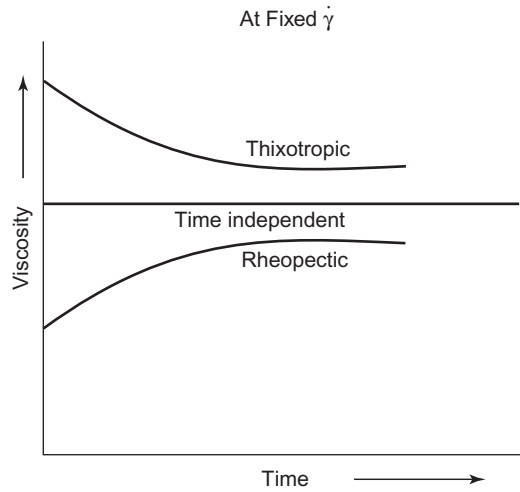


**FIGURE 4.29**

Viscosity–time relations for time-dependent fluids.

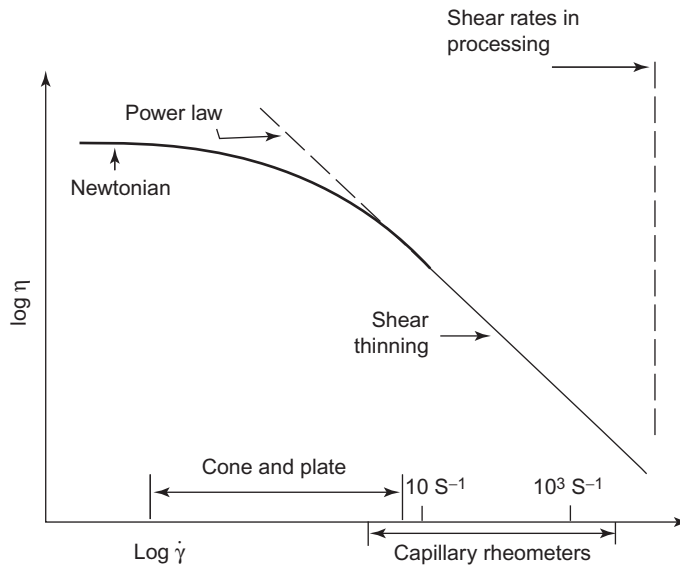


**FIGURE 4.30**

Typical rheometer shear rate ranges and polymer melt flow curve. The lower shear rate region of the flow curve exhibits viscosities that appear to be independent of  $\dot{\gamma}$ . This is the lower Newtonian region.

representative shear rate ranges for cone-and-plate and capillary rheometers. The last viscometer type, which bears a superficial resemblance to the orifice in an extruder or injection molder, is the most widely used and will be the only type considered in this nonspecialized text.

Equation (4-90) [cf. Eq. (3-87)] gives the relation between flow rate and viscosity for a fluid under pressure  $P$  in a tube with radius  $r$  and length  $l$ . In such a device the apparent shear stress,  $\tau_a = Pr/2l$ ; and the apparent shear rate,  $\dot{\gamma}_a = 4Q/\pi r^3$ , where  $Q$ , the volumetric flow rate, is simply the  $Q/t$  term of Eq. (3-87). That is,

$$\eta = \frac{\pi Pr^4 t}{8Ql} = \frac{Pr/2l}{4Q/\pi r^3} = \frac{\tau_a}{\dot{\gamma}_a} \quad (4-90)$$

The shear stress and shear rate here are termed apparent, as distinguished from the respective true values at the capillary wall,  $\tau_w$  and  $\dot{\gamma}_w$ . The Bagley correction to the shear stress allows for pressure losses incurred primarily by accelerating the polymer from the wider rheometer barrel into the narrower capillary entrance [24]. It is measured by using a minimum of two dies, with identical radii and different lengths. The pressure drop, at a given apparent shear rate, is plotted against the  $l/r$  ratio of the dies, as shown in Fig. 4.31. The absolute values of the negative intercepts on the  $l/r$  axis are the Bagley end-corrections,  $e$ . The true shear stress at each shear rate is given by

$$\tau_w = \frac{P}{[2\frac{l}{r} + e]} \quad (4-91)$$

Alternatively,  $\tau_w$  can be measured directly by using a single long capillary with  $l/r$  about 40. The velocity gradient in Fig. 3-6 is assumed to be parabolic, but this is true strictly only for Newtonian fluids. The Rabinowitsch equation [25] corrects for this discrepancy in non-Newtonian flow, such as that of most polymer melts:

$$\dot{\gamma}_w = \left[ \frac{3n+1}{4n} \right] \frac{4Q}{\pi r^3} \quad (4-92)$$

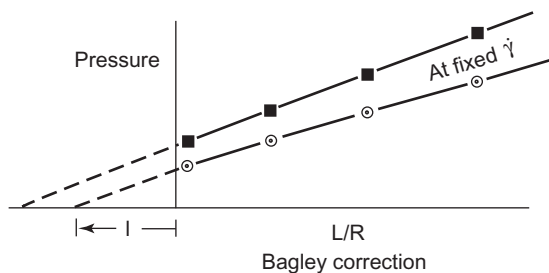


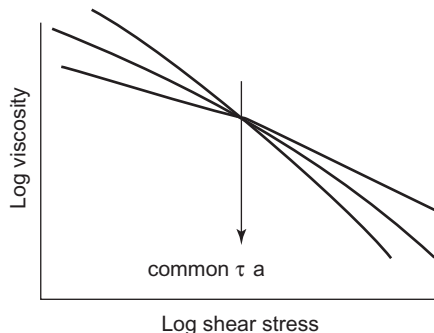
FIGURE 4.31

Bagley end correction plot.

where  $n$  is the power law index mentioned earlier. Application of the Bagley and Rabinowitsch corrections (in that order) converts the apparent flow curve from capillary rheometer measurements to a true viscous flow curve such as would be obtained from a cone-and-plate rheometer. However, this manipulation has sacrificed all information on elastic properties of the polymer fluid and is not useful for prediction of the onset of many processing phenomena, which we will now consider.

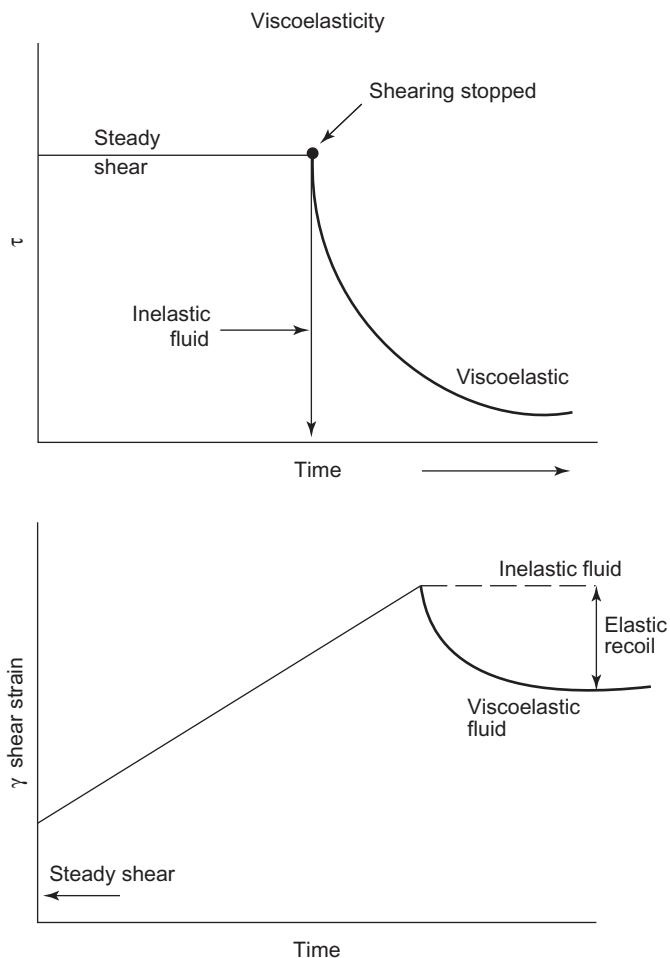
Measurements made under standardized temperature and pressure conditions from a simple capillary rheometer and orifice of stipulated dimensions provide *melt flow index* (MFI) or *melt index* characteristics of many thermoplastics. The units of MFI are grams output/10 min extrusion time. The procedure, which amounts to a measurement of flow rate at a standardized value of  $\tau_a$ , is very widely used for quality and production control of polyolefins, styrenics, and other commodity polymers. A lower MFI shows that the polymer is more viscous under the conditions of the measurement. This parameter can be shown to be inversely related to a power of an average molecular weight of the material [26]  $[\text{MFI}]^{-1} \propto M_w^{3.4-4.7}$ . MFI, which is easy to measure, is often taken to be an inverse token of polymer molecular size. The problem with this assumption is that MFI, or  $\eta_a$  for that matter, scales with average molecular weight only so long as the molecular weight distribution shape is invariant. This assumption is useful then for consideration of the effects of variations in a particular polymerization process but may be prone to error when comparing products from different sources.

A more serious deficiency resides in reliance on MFI to characterize different polymers. No single rheological property can be expected to provide a complete prediction of the properties of a complex material like a thermoplastic polymer. Figure 4.32 shows  $\log \eta_a - \log \tau_a$  flow curves for polymers having the same melt index, at the intersection of the curves, but very different viscosities at higher shear stress where the materials are extruded or molded. This is the main reason why MFI is repeatedly condemned by purer practitioners of our profession. The parameter is locked into industrial practice, however, and is unlikely to be displaced.



**FIGURE 4.32**

Apparent flow curves of different polymers with the same MFI (at the intersection point).

**FIGURE 4.33**

Comparisons of inelastic and viscoelastic behavior on the cessation of steady shearing.

Viscoelasticity was introduced in [Section 4.7](#). A polymer example may be useful by way of recapitulation. Imagine a polymer melt or solution confined in the aperture between two parallel plates to which it adheres. One plate is rotated at a constant rate, while the other is held stationary. [Figure 4.33a](#) shows the time dependence of the shear stress after the rotation has been stopped.  $\tau$  decays immediately to zero for an inelastic fluid but the decrease in stress is much more gradual if the material is viscoelastic. In some cases, the residual stresses may not reach zero, as in molded or extruded thermoplastics that have been quenched from the molten state. Such articles contain molded-in stresses that are relieved

by gradual decay over time, resulting in warpage of the part. Figure 4.33b sketches the dependence of the deformation once the steady shearing has stopped. An inelastic fluid maintains the final strain level, while a viscoelastic substance will undergo some elastic recoil.

Whether a polymer exhibits elastic as well as viscous behavior depends in part on the time scale of the imposition of a load or deformation compared to the characteristic response time of the material. This concept is expressed in the dimensionless Deborah number:

$$N_{\text{Deb}} = \frac{\text{response time of material}}{\text{time scale of process}}$$

(This parameter was named after the prophetess Deborah to whom Psalm 114 has been ascribed. This song states correctly that even mountains flow during the infinite observation time of the Lord, viz., “*The mountains skipped like rams, The hills like lambs.*”) The process is primarily elastic if  $N_{\text{Deb}} > 1$  and essentially viscous if  $N_{\text{Deb}} < 1$ . The response time of the polymer, and its tendency to behave elastically, will increase with higher molecular weight and skewing of the molecular weight distribution toward larger species.

A number of polymer melt phenomena reveal elastic performance [27]. A common example is extrudate swell (or die swell), in which the cross section of an extruded profile is observed to be larger than that of the orifice from which it was produced. Melt elasticity is required during extrusion coating operations where the molten polymer sheet is pulled out of the sheet die of the extruder by a moving substrate of paper or metal foil. Since the final laminate must be edge-trimmed it is highly desirable that the edges of the polymer match those of the substrate without excessive edge waviness or tearing. This requires a good degree of melt cohesion provided by intermolecular entanglements which also promote elasticity. Other elasticity-related phenomena include undesirable extrudate surface defects, called melt fracture and sharkskin, which appear with some polymers as extrusion speeds are increased.

A number of modern devices provide accurate measurements of both viscous and elastic properties (although some have limited shear rate ranges). An inexact but very convenient indicator of relative elasticity is extrudate swell which is inferred from the ratio of the diameter of the leading edge of a circular extrudate to that of the corresponding orifice. Since MFI is routinely measured, its limited value can be augmented by concurrent die swell data. As an example, polyethylenes intended for extrusion coating should be monitored for minimum die swell, at given melt index, while polymers for high-speed wire covering require maximum die swell values, which can be set by experience.

The emphasis to this point has been on viscous behavior in shearing modes of deformation. However, any operation that reduces the thickness of a polymeric liquid must do so through deformations that are partly extensional and partly shear. In many cases polymers respond very differently to shear and to extension. A prime industrial example involves low-density and linear low-density

polyethylenes, i.e., LDPE and LLDPE, respectively (Section 11.5.3). LDPE grades intended for extrusion into packaging film have relatively low shear viscosities and high elongational viscosities. As a result, extrusion of tubular film involves reasonable power requirements and stable inflated film “bubbles” between the die and film take-off. LLDPEs of comparable MFIs require much more power to extrude. Their melts can, however, be drawn down to much thinner gauges (an advantage), but the tubular film bubbles are more prone to wobble and tear (a disadvantage). The best of both worlds can be realized by blending minor proportions of selected LDPEs into LLDPEs.

When problems occur during polymer processing it is necessary to perform at least a preliminary analysis of the particular fabrication process. Experiments on production equipment are time-consuming, difficult to control and expensive. Therefore, equivalent laboratory experiments are very desirable. Ideally, one would be able to analyze the production process in terms of fundamental physical quantities and measure these with rheological equipment. It is necessary to make sure that the laboratory measurements correspond to the actual production process and to select the rheological characteristics that bear on the particular problem. That is to say, do not measure viscosity to try to get information about a phenomenon that is affected mainly by the elastic character of the material. Note in this connection that most laboratory data are obtained from steady-state measurements, while the polymers in some processes never reach equilibrium condition. (The ink in a high-speed printing operation is a good example.) If this rheological analysis is not feasible the production process can sometimes be simulated on a small, simplified scale, while paying attention to the features that are critical in the simulation.

There are a number of fine recent rheological references [28–30] that should be consulted for more details than can be considered in an introductory text.

---

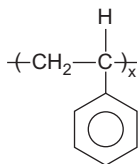
## 4.14 Effects of Fabrication Processes

An important difference between thermoplastics and other materials of construction lies in the strong influence of fabrication details on the mechanical properties of plastic articles. This is exhibited in the pattern of frozen-in orientation and fabrication stresses. The manufacturing process can also have marked effects on crystalline texture and qualities of products made from semicrystalline polymers. Orientation generally produces enhanced stiffness and strength in the stretch direction and weakness in the transverse direction. In semi-crystalline polymers, the final structure is sensitive to the temperature–time sequence of the forming and subsequent cooling operations and to the presence or absence of orientation during cooling. Different properties are produced by stretching a crystallized sample at temperatures between  $T_g$  and  $T_m$ , or by orienting the molten polymer before crystallizing the product.

In summary, the final properties of thermoplastic articles depend both on the molecular structure of the polymer and on the details of the fabrication operations. This is a disadvantage, in one sense, since it makes product design more complicated than with other materials that are less history-dependent. On the other hand, this feature confers an important advantage on plastics because fabrication particulars are additional parameters that can be exploited to vary the costs or balance of properties of the products.

## PROBLEMS

- 4-1 Nylon-6,6 can be made into articles with tensile strengths around 12,000 psi or into other articles with tensile strengths around 120,000 psi. What is the basic difference in the processes used to form these two different articles? Why do polyisobutene properties not respond in the same manner to different forming operations?
- 4-2 Suggest a chemical change and/or a process to raise the softening temperature of articles.



- 4-3 (a) Calculate the fraction of crystallinity of polyethylene samples with densities at 20 °C of 926, 940, and 955 kg/m<sup>3</sup>. Take the specific volume of crystalline polyethylene as  $0.989 \times 10^{-3} \text{ m}^3/\text{kg}$  and that of amorphous polyethylene as  $1.160 \times 10^{-3} \text{ m}^3/\text{kg}$ . (b) What assumption did you make in this calculation?
- 4-4 The melting points of linear C<sub>n</sub>H<sub>2n+2</sub> molecules can be fitted to the empirical equation

$$T_m(\text{K}) = 1000/(2.4 + 17n^{-1})$$

Plot the graph of  $T_m$  against  $n$  using the equation and compare the observed values of  $T_m$  listed below with the curve. Determine the equilibrium melting point  $T_m^0$  for high-density polyethylene.

$n$	8	10	12	14	16	24	32
$T_m$ (°C)	-56.8	-29.7	-9.7	2.5	14.7	47.6	67

Given that  $T_m = T_m^0 \left(1 - \frac{2\gamma_e}{\Delta H}\right)$ , determine  $T_m$  for the high-density polyethylene containing lamella with an average thickness ( $l$ ) of 12.0 nm. Take  $\gamma_e = 0.0874 \text{ J/m}^2$  and  $\Delta H = 279 \text{ MJ/m}^3$ .

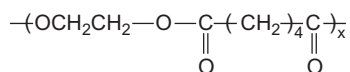
- 4-5 The Clausius–Clapeyron equation for the effects of pressure on an equilibrium temperature is

$$dP/dT = \Delta H/T \Delta V$$

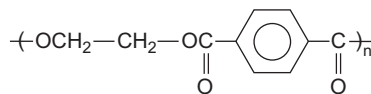
where  $\Delta H$  is the enthalpy change and  $\Delta V$  is the volume change associated with a phase change. Calculate the melting temperature for polyethylene in an injection molding operation under a hydrostatic pressure of 80 MPa. Take  $\Delta H = 7.79 \text{ kJ/mol}$  of ethylene repeat units and  $T_m = 143.5 \text{ }^\circ\text{C}$  at 1 atm.

- 4-6 Which of the following polymers would you expect to have a lower glass transition temperature? Which would have a higher melting point? Explain why. (Assume equal degrees of polymerization.)

(a)



(b)



- 4-7 Estimate the glass transition temperature of a copolymer of vinyl chloride and vinyl acetate containing 10 wt% vinyl acetate. The  $T_g$ 's of the homopolymers are listed in Table 4.2.
- 4-8 According to the Arrhenius equation,  $\ln a_T$  and temperature  $T$  are related as follows:

$$\ln a_T = \frac{E}{R} \left( \frac{1}{T} - \frac{1}{T_0} \right)$$

where  $E$  is the activation energy for the viscoelastic relaxation and  $R$  is the gas constant (8.314 J/mol K).

- (a) Obtain an analytical expression for the activation energy for materials exhibiting viscoelastic behavior that can be described by the WLF equation in terms of constants  $C_1$  and  $C_2$  and  $T_0 = T_g$ .

- (b) Given that  $C_1 = 17.4$  and  $C_2 = 51.6$ , determine the activation energy (kJ/mol) at  $T_g$  for  $T_g = 200$  K.
- (c) If the viscosity of the polymer at  $T_g$  is around  $10^{13}$  poise (10 poise = 1 Pa·s), estimate the shift factor and viscosity (poise)  $50^\circ\text{C}$  above  $T_g$ .

- 4-9** If we consider a polymer to be made of only chain ends and chain mid-dles, show that the following equation may be obtained from the Flory–Fox equation ( $T_g = T_g^\infty - u/M_n$ ):

$$T_g = T_g^\infty - \frac{uw_e}{M_e}$$

where  $w_e$  is the mass fraction of the chain ends and  $M_e$  is the mass of chain ends per mole of chains. One of the equations used to predict glass transition temperature depression due to the incorporation of a small amount of solvent in a polymer is

$$T_g = T_{g,p}w_p + T_{g,s}w_s + Kw_pw_s$$

where subscripts  $p$  and  $s$  refer to the polymer and the solvent, respectively, and  $K$  is a constant. Rearrange the above equation into the following form by considering chain ends as solvent

$$T_g = T_{g,p} - \frac{uw_e}{M_e}$$

where  $M_e$  is the mass of the polymer per mole of the polymer solution. Note that  $u$  here and  $u$  that appeared in the Flory–Fox equation and in the equation that relates  $T_g$  and the mass fraction of chain ends are not the same constant.

- 4-10** A rubber has a shear modulus of  $10^7$  dyn/cm<sup>2</sup> and a Poisson's ratio of 0.49 at room temperature. A load of 5 kg is applied to a strip of this material which is 10 cm long, 0.5 cm wide, and 0.25 cm thick. How much will the specimen elongate?
- 4-11** If a bar of elastic material is held at constant length  $L$  while temperature  $T$  is raised, show that the force changes at the rate given by

$$\left(\frac{\partial f}{\partial T}\right)_L = -\left(\frac{\partial S}{\partial L}\right)_T$$

where  $S$  is the entropy of the bar, if it is assumed that the stress-free length is independent of temperature (i.e., free thermal expansion is ignored). In practice, when this experiment is conducted on polymers in the rubbery state, it is found that  $(\partial f/\partial T)_L$  is negative at small extensions but is positive at large extensions. Explain this.

- 4-12** An ideal rubber band is stretched to a length of 15.0 cm from its original length of 6.00 cm. It is found that the stress at this length increases by an increment of  $1.5 \times 10^5$  Pa when the temperature is raised  $5^\circ\text{C}$  (from  $27^\circ\text{C}$  up to  $32^\circ\text{C}$ ). What modulus ( $E = \sigma/\epsilon$ ) should we expect to measure at 1% elongation at  $27^\circ\text{C}$ ? Neglect any changes in volume with temperature. Do all the calculations using the engineering tensile stress equation.
- 4-13** About one out of every 150 chain carbon atoms is cross-linked in a typical natural rubber (*cis*-polyisoprene) compound with good properties. The density of such a vulcanizate is  $0.97\text{ g cm}^{-3}$  at  $25^\circ\text{C}$ . The gas constant  $R = 8.3 \times 10^7\text{ ergs mol}^{-1}\text{K}^{-1} = 1.987\text{ cal mol}^{-1}\text{K}^{-1}$ . Estimate the modulus of the sample at low extensions.
- 4-14** The work done by an external force applied on a piece of ideal rubber containing  $\nu$  network chains is given by

$$w = \frac{\nu k_B T}{2} \frac{\langle r^2 \rangle_i}{\langle r^2 \rangle_0} (\Lambda_x^2 + \Lambda_y^2 + \Lambda_z^2 - 3)$$

where  $k_B$  is the Boltzmann constant ( $1.38 \times 10^{-23}\text{ J/K}$ );  $\langle r^2 \rangle_i$  and  $\langle r^2 \rangle_0$  are the mean square end-to-end distances of the network chains in and out of the network; and  $\Lambda_x$ ,  $\Lambda_y$ , and  $\Lambda_z$  are the extension ratios in the  $x$ ,  $y$ , and  $z$  directions. A bar of ideal rubber with square in cross-section containing  $6 \times 10^{20}$  network chains is extended uniaxially at  $20^\circ\text{C}$  until its length is double the initial length. Assuming that  $\langle r^2 \rangle_i = 0.8 \langle r^2 \rangle_0$  and  $\Lambda_x \Lambda_y \Lambda_z = 1$ ,

- (a) Calculate the heat gained or lost;  
 (b) Determine the entropy change of the process;  
 (c) Comment on the result you obtained in part (b).
- 4-15** The raw data from a tensile test are obtained in terms of force and corresponding elongation for a test specimen of given dimensions. The area under such a force–elongation curve can be equated to the impact strength of an isotropic polymer specimen if the tensile test is performed at impact speeds. Show that this area is proportional to the work necessary to rupture the sample.
- 4-16** The stress relaxation modulus for a polyisobutene sample at  $0^\circ\text{C}$  is  $2.5 \times 10^5\text{ N/m}^2$ . The stress here is measured 10 min after imposition of a fixed deformation. Use the WLF equation (Eq. 4-72) to estimate the temperature at which the relaxation modulus is  $2.5 \times 10^5\text{ N/m}^2$  for a measuring time of 1 min.
- 4-17** The stress relaxation behavior of a particular grade of polymer under constant strain is given by the following expression:

$$\tau(t) = G\gamma_0 e^{-t/\lambda} + \tau_0$$

where  $G$  is a constant,  $\gamma_0$  is the initial strain imposed on the polymer,  $\tau_0$  is the residue stress that is related to  $\gamma_0$  in the form of  $\tau_0 = \gamma_0^2$ , and  $\lambda$  is the relaxation time.

- (a) What is the relaxation modulus of the polymer?
- (b) What are the initial and final stresses?
- (c) Given that  $G = 0.8$  MPa and  $\gamma_0 = 0.15$ , calculate the percentage of the original stress that has decayed when  $t = \lambda$ .
- (d) It has been found that the above model is a better model than the Maxwell model to describe the stress of the polymer, especially at long times. Why?

- 4-18** The complex shear strain  $\gamma^*$  and complex shear stress  $\tau^*$  are given by the following expressions:

$$\gamma^* = \gamma_0 e^{i\omega t}; \quad \tau^* = \tau_0 e^{i(\omega t + \delta)}$$

Based upon the above expressions, show that the real and imaginary parts of the complex shear compliance  $J^*$  are given by the following equations:

$$J' = \frac{\gamma_0}{\tau_0} \cos \delta; \quad J'' = \frac{\gamma_0}{\tau_0} \sin \delta$$

Also show that  $J''/J' = \tan \delta$ . If the magnitudes of  $\gamma^*$  and  $\tau^*$  are 10% and  $10^5$  Pa and the phase angle of the material is  $45^\circ$ , calculate the amount of energy that is dissipated per full cycle of deformation ( $J/m^3$ ).

- 4-19** Consider a sinusoidal shear strain with angular frequency  $\omega$  and strain amplitude  $\gamma_0$  (i.e.,  $\gamma(t) = \gamma_0 \sin(\omega t)$ ).
- (a) What is the corresponding time dependent shear stress for a perfectly elastic material that has a shear modulus of  $G$  and is subjected to the above sinusoidal shear strain?
  - (b) Show that the shear stress of a Newtonian liquid with a viscosity of  $\eta$  still oscillates with the same angular frequency but is out-of-phase with the sinusoidal shear strain by  $\pi/2$ .
  - (c) What is the time-dependent shear stress of a viscoelastic material with a stress amplitude  $\sigma_0$  and in which stress leads the strain by a phase angle  $\delta$ ?
  - (d) What is the corresponding expression of the above described sinusoidal shear strain written in the complex number form?
  - (e) If a sinusoidal shear strain is in the form of  $\gamma(t) = \gamma_0 e^{i\omega t}$ , determine the magnitudes of the shear strains and the corresponding shear stresses for a viscoelastic material when  $\omega t = 0, \pi/2, \pi, 3\pi/2, \text{ and } 2\pi$ . Note that the time-dependent shear stress has a stress amplitude  $\sigma_0$  and that its stress leads the strain by a phase angle  $\delta$ .
  - (f) The following expression shows the complex compliance of a viscoelastic material which is subjected to a sinusoidal shear strain in the

form of  $\gamma(t) = \gamma_0 e^{i\omega t}$ . Comment on the viscoelastic behavior of the material as a function of angular frequency.

$$J^* = J' - iJ'' = \frac{G}{G^2 + \eta^2\omega^2} - i \frac{\eta\omega}{G^2 + \eta^2\omega^2}$$

- 4-20** A Maxwell model (Eq. 4-59, Fig. 4.18b) is being deformed at a constant rate  $d\gamma/dt = C$ . What is the stress on the element  $[\sigma(t)]$  at a time  $t$  after the imposition of the fixed straining rate? Express your answer in terms of the constants  $G$  and  $\eta$  of the Maxwell element and the strain  $\gamma(t)$  which corresponds to  $\sigma(t)$ .
- 4-21** Commercial polymer films are usually produced with some orientation. The orientation is generally different in the longitudinal (machine) direction than in the transverse direction. How could you tell which is the machine direction from a stress-strain test? (*Hint*: Refer back to the effects of orientation mentioned in Section 1.8.)
- 4-22** The hoop stress,  $\sigma_h$ , at the outer surface of a pipe with internal pressure  $P$ , outside diameter  $d_1$ , and inside diameter  $d_2$  is

$$\sigma_h = \frac{2Pd_2^2}{d_1^2 - d_2^2}$$

A well-made PVC pipe has outside diameter 150 mm and wall thickness 15 mm. Measurements on this pipe give  $K_{Ic} = 2.4 \text{ MPa} \cdot \text{m}^{1/2}$  and yield stress,  $\sigma_y = 50 \text{ MN} \cdot \text{m}^{-2}$ . Assume that the largest flaws are 100- $\mu\text{m}$  cracks and that the calibration factor for the specimens used to measure fracture toughness is 1.12. The pipe is subjected to a test in which the internal pressure is gradually raised until the pipe fails. Will the pipe fail by yielding or brittle fracture in this burst test? At what pressure will the pipe rupture?

---

## References

- [1] T. Bremner, A. Rudin, J. Polym. Sci., Phys. Ed. 30 (1992) 1247.
- [2] T.A. Kavassalis, P.R. Sundararajan, Macromolecules 26 (1993) 4146.
- [3] V.P. Privalko, Y.S. Lipatov, Makromol. Chem. 175 (1974) 641.
- [4] M. Gordon, High Polymers, Addison-Wesley, Reading, MA, 1963.
- [5] H. Mark, ChemTech, 220 (April 1984).
- [6] L.R.G. Treloar, The Physics of Rubber Elasticity, third ed., Oxford (Clarendon) University Press, London and New York, 1975.
- [7] M.L. Williams, R.F. Landel, J.D. Ferry, J. Am. Chem. Soc. 77 (1955) 3701.
- [8] K.H. Illers, H. Breuer, Kolloid. Z. 17b (1961) 110.
- [9] A.M. Donald, E.J. Kramer, J. Polym. Sci., Polym. Phys. Ed. 20 (1982) 899.

- [10] S. Hashemi, J.G. Williams, *Polym., Eng. Sci.* 16 (1986) 760.
- [11] A.C. Yang, E.J. Kramer, *Macromolecules* 19 (1986) 2010.
- [12] B.Z. Jang, D.R. Uhlmann, J.B. Vander Sande, *J. Appl. Polym. Sci.* 29 (1984) 3409.
- [13] K.C.E. Lee, Ph.D. Thesis, University of Waterloo, 1995.
- [14] L. Morbitzer, *J. Appl. Polym. Sci.* 20 (1976) 2691.
- [15] A.E. Griffith, *Phil. Trans. Roy. Soc. A* 221 (1921) 163.
- [16] G.R. Irwin, in *Fracturing of Metals*, p. 147. American Society of Metals, Cleveland, 1948.
- [17] ASTM Standard E399. American Society for Testing Materials, Philadelphia, D.P. Rooke, D.J. Cartwright, *Compendium of Stress Intensity Factors*, HMSO, London, 1976.
- [18] E. Plati, J. Williams, *Polym. Eng. Sci.* 15 (1975) 470.
- [19] R.W. Truss, *Plast. Rubber Process. Appl.* 10 (1988) 1.
- [20] N.G. McCrum, C.P. Buckley, C.B. Bucknall, *Principles of Polymer Engineering*, Oxford University Press, Oxford, 1990.
- [21] S. Turner, G. Dean, *Plast. Rubber Process. Appl.* 14 (1990) 137.
- [22] D.R. Moore, *Polymer Testing* 5 (1985) 255.
- [23] R.M. Crieens, H.G. Mosle, *Soc. Plast. Eng. Antec.* 40 (1982) 22.
- [24] E.B. Bagley, *J. Appl. Phys.* 28 (1957) 624.
- [25] B. Rabinowitsch, *Z. Physik. Chem.* A145 (1929) 1.
- [26] T. Bremner, D.G. Cook, A. Rudin, *J. Appl. Poly. Sci.* 41 (1990) 161743, 1773 (1991).
- [27] E.B. Bagley, H.P. Schreiber, in: F.R. Eirich (Ed.), *Rheology*, Vol. 5, Academic Press, New York, 1969.
- [28] F.N. Cogswell, *Polymer Melt Rheology*, Woodhead Publishing, Cambridge, England, 1997.
- [29] J.M. Dealy, *Rheometers for Molten Plastics*, Van Nostrand Reinhold, New York, 1982.
- [30] J.M. Dealy, K.F. Wissbrun, *Melt Rheology and Its Role in Plastics Processing*, Van Nostrand Reinhold, New York, 1990.